RADIAL SPREADING OF VERTICAL BUOYANT JETS IN SHALLOW WATER

by

MICHAEL RAY MACLATCHY

B.A.Sc, The University of British Columbia, 1991

A THESIS SUBMITTED IN PARTIAL FULFILLMENT OF THE REQUIREMENTS
FOR THE DEGREE OF MASTER OF APPLIED SCIENCE

in

THE FACULTY OF GRADUATE STUDIES

(Department of Civil Engineering)

We accept this thesis as conforming to the required standard

THE UNIVERSITY OF BRITISH COLUMBIA

August 1993

(Signature)

Department of _Civil Engineering_

The University of British Columbia
Vancouver, Canada

Date _August 19 1993_

DE-6 (2/88)

Abstract

Many wastewaters are discharged from single vertical outlets located at the bottom of shallow water bodies. Often these effluents are buoyant with respect to the receiving environment. In many jurisdictions, regulations require that a certain dilution is achieved within a specified mixing zone. In shallow water it is likely that a portion of this dilution will have to be achieved in the radially spreading surface region of the jet. The degree of dilution obtained in the radial surface buoyant jet region will depend upon the buoyancy and velocity of the effluent, and the depth of water available. Prior to the installation of an outfall, the dilution that will be achieved and behaviour of the flow must be modeled in developing the design to meet regulatory and other requirements. Unfortunately, radially spreading flows are not clearly understood, and their behaviour is the subject of some controversy.

This study was intended to identify the details of the structure of the radially spreading upper layer associated with the discharge of a vertical buoyant jet in shallow water. Collection and analysis of detailed numerical data was not the focus or intent of this study, flow visualization was relied upon to investigate the radially spreading surface flow. Experiments to study the mechanisms of the radially spreading surface flow were conducted with a series of vertical buoyant jets discharged into a shallow tank. This experimental tank was specially designed to simulate an infinite ambient, and avoid downstream control effects. A range of flow rates and port diameters were utilized to determine the nature of the flow structure in the surface region. Flow visualization was used to examine the flow and obtain an understanding of the mechanisms present to aid in modeling.

Four regions of flow are present when a buoyant jet is discharged vertically in shallow water. The first of these is the vertical buoyant jet region, in which the vertical jet is entraining fluid as the flow moves upward to the surface. Next is a surface impingement

region, where the vertical flow arrives at the surface, and is redirected to an outward, radially spreading surface flow. The first of two surface regions is the radial buoyant jet region, in which the momentum of the fluid dominates. This study determined that in this region the surface flow exists as a series of billows or vortices into which ambient fluid is entrained as they grow and move radially outward. Eventually this flow will have spread out, and entrained enough fluid, that the interfacial shear will decrease to the point where buoyancy will dominate. The large scale billows will collapse, to be replaced by smaller less vigorous interfacial instabilities, as the second surface region, the radial buoyant plume region, is entered. Contrary to the assumptions made by some researchers, no radial internal hydraulic jumps were detected in the radially spreading surface flow regions.

Table of Contents

List of Tables
(Appendix A)

List of Figures
(Appendix B)

Acknowledgments

For his constant encouragement and constructive supervision, I would like to thank my thesis supervisor, Dr. G. A. Lawrence. I would also like to thank Kurt Nielson, of the Civil Engineering Hydraulics Laboratory, for the construction of the experimental apparatus used in this study. A special thanks goes to Jason Vine for his assistance with the scientific laser during experiments, and in the darkroom developing film.

Chapter 1

Introduction

Many wastewater discharges, such as pulp mill effluents and cooling water from thermal power plants, are buoyant with respect to the receiving water that they are entering. The effluents are frequently released as vertical discharges located at the bottom of shallow water bodies. Such discharges pose a concern from an environmental standpoint. Contaminants or heat may be present, with the potential for a negative impact on the receiving environment. Depending upon the location, and regulatory requirements, it is often necessary to achieve a required dilution within a certain distance of the point of discharge. In shallow water the degree of dilution will be greatly influenced by the depth available in which the jet may entrain fluid. Once surface impingement occurs radial spreading of the jet may account for additional dilution. The extent to which this additional dilution occurs will depend on such factors as the buoyancy and velocity of the effluent, and the relative proportion of the depth occupied by the surface layer. Eventually, as the distance from the discharge point increases, the initial momentum of the discharge will be of less importance, and the behaviour of the flow will become plume like, buoyancy effects will dominate.

While most real situations will involve the presence of ambient currents, the basic situation in which the ambient is stagnant has considerable relevance, both as a fundamental case, and in situations where the ambient currents are relatively small with respect to the velocities in the radially spreading surface flow. Models for predicting the dilution and behaviour of vertical round buoyant jets in shallow water have been presented by Lee & Jirka (1981), Wright et. al. (1991) and Lawrence & Bratkovitch (1993), to name a few. These models draw on earlier work, such as Crow & Champagne (1971), Abraham (1965), Wilkinson & Wood (1971), and Chen (1980). Experimental investigation has

largely been limited to a confirmation and calibration of the bulk parameters of these models. Detailed examination of the physical mechanisms of the surface flow has not been undertaken to any great extent. Certain of the models have been based on assumptions, adopted for mathematical convenience, as to what is occurring in the radial surface flow. In order to better understand the behaviour of the radial surface flow and to formulate better models, the present study will undertake to investigate the behaviour and mechanisms of the radial surface flow. The main emphasis of this study will be to examine the radially spreading surface flow, and identify the structures present by flow visualization techniques. Detailed analyisis of hard numerical data, such as the velocities in the surface spreading layer, or the dilution and entrainment occurring, will be undertaken in future investigations.

Most researchers have recognized that there are two basic parameters that determine the behaviour of a vertical buoyant jet surfacing in stagnant shallow water, these being the densimetric Froude number, and the ratio of the depth of ambient water to the jet orifice diameter, H/D. Three distinct regions of flow have been identified in the near-field, though the exact behaviour of the surface flow in the near-field is open to debate. Basic relationships used to describe the velocity and concentration profiles, and dilution of vertical buoyant jets (Fischer et al., 1979, and List, 1982) are presented in Chapter 2, as well as a review of literature regarding vertical buoyant jets discharged in shallow water.

Experiments to investigate the behaviour of the surface flow associated with the discharge of a vertical buoyant jet in shallow water are discussed in Chapter 3. A thermally buoyant jet was discharged into cold ambient water, which was constantly being replenished to replace entrained fluid. Visualization of the mechanisms in the surface flow was accomplished using a sheet of laser light, and fluorescent dye injected into the jet fluid. Chapter 3 contains a description of the design of the experimental apparatus, and details of the experimental procedure. Results and discussion are presented in Chapter 4.

Conclusions and recommendations arising out of this study are presented in Chapter 5.

The results of this thesis will be of use in increasing the understanding of radial surface flow. A large number of discharges exist as single vertical buoyant jets located at the bottom of nearly stagnant shallow water. In these cases, as long as ambient currents are small relative to the velocities of the radially spreading flow in the near-field, the information obtained from this study should assist in predicting the flow conditions and mixing which will occur. Refinement of predictive models used to aid in design of outfalls will hopefully arise out of this study.

Chapter 2

Literature Review

While a number of papers have presented models of the dilution which occurs in the surface regions of a vertical buoyant jet in shallow water, relatively little work has been undertaken to investigate the mixing mechanisms, and the manner in which the transition from near-field to far-field occurs. This review will start by considering the basic jet and plume parameters, and the simple relationships which exist for dilution, and velocity and concentration profiles. Then a number of models regarding the discharge of vertical buoyant jets into shallow water will be focused on, with emphasis on the assumptions made in developing the models presented. Where experimental results exist, these will be discussed, particularly where hydraulic experiments provide insight into the mechanisms involved. Where investigations regarding other situations, such as for plane vertical jets or two layer channel flow, contain useful results they will be discussed.

The simple case of a vertical buoyant jet discharging into deep stagnant ambient water has received considerable attention, an introduction to this case, as well as the case of buoyant plumes, is presented in Fischer et al. (1979). Fischer et al. (1979) also presents a general approach for the case of a vertical jet or plume in deep flowing water. List (1982) provides an overview of the basic characteristics and parameters for buoyant jets and plumes. Jirka (1981) presents an approach to the problem of vertical buoyant jets discharged into shallow water.

This review is divided into two major parts. In the first part the basic parameters which describe jets and plumes are presented and discussed. The second part covers the theory of buoyant jets in shallow water, and the available results of investigations of the mixing mechanisms.

2. 1. Basic Jet and Plume Parameters

The behaviour of a jet or plume discharged into a fluid is governed by three general categories of parameters. These parameters are environmental, which relates to the conditions in the ambient fluid; geometrical, which deal with the geometric relationship between the jet and the ambient fluid; and jet parameters which are the specific properties of the jet. Examples of environmental conditions are the density stratification, flow velocities, and degree of turbulence in the ambient fluid. Geometrical parameters of importance include the depth of submergence of the jet, angle of the jet to the horizontal, or angle of the jet to the flow in the ambient. Significant jet (or plume) parameters include the jet velocity, total discharge, and density deficit between the jet and the ambient fluid.

Making use of the definitions in Fischer et al. (1979), there are three expressions that are useful in describing the conditions in a jet:

$$\text{Volume flux,} \qquad \mu = \int_A u\,dA \qquad\qquad (2.\ 1)$$

$$\text{Momentum flux,} \qquad m = \int_A u^2\,dA \qquad\qquad (2.\ 2)$$

$$\text{Buoyancy flux,} \qquad \beta = \int_A g'u\,dA \qquad\qquad (2.\ 3)$$

Where: A = cross sectional area of jet.

u = time averaged velocity in axial direction.

μ = specific mass flux or volume flux.

m = specific momentum flux.

β = the specific buoyant or submerged weight of the fluid passing through a cross section per unit time. The specific buoyancy flux.

g' = $(\Delta\rho/\rho)g$, effective gravitational acceleration.

These quantities will vary with location in the jet as fluid is entrained and velocities decrease (discussed later). For purposes of determining how the jet will behave it is often

more convenient to state these quantities in terms of the initial jet conditions. In terms of the initial jet conditions the equivalent expressions to equations 2.1 to 2.3 above are:

$$Q = \frac{\pi}{4} D^2 U \qquad (2.4)$$

$$M = \frac{\pi}{4} D^2 U^2 \qquad (2.5)$$

$$B = g'_o Q \qquad (2.6)$$

Where: Q = initial volume flow rate (at jet exit).

M = initial mass flux rate.

B = initial buoyancy flux rate.

g'_o = initial effective gravitational acceleration.

Note that these expressions are for round jets, similar expressions are possible for other jet configurations. From research, it has been determined that the three initial parameters, Q, M, and B will govern the behaviour of round buoyant jets as long as the jet is fully turbulent, that is, if the jet Reynolds number is greater than about 4000. If this condition is met, other factors will have relatively little significance in determining the behaviour of the jet. We will now discuss the behaviour, and the relationships used to describe the behaviour, of pure jets, pure plumes and buoyant jets.

2. 1. 1.   Pure Jets

Upon entering the ambient fluid, a shear layer will form between the jet and the ambient fluid. The behaviour of the jet may be broken into two distinct zones, the <u>Zone of Flow Establishment</u> (ZFE), and the <u>Zone of Established Flow</u> (ZEF), refer to Figure 2.1. Within the first zone (ZFE), the shear forces generated by the interaction of the jet and the ambient fluid have not penetrated into the center of the jet, and there exists a jet core in which the velocity remains equal to the jet exit velocity. After a short distance from the jet exit, approximately six to seven port diameters (z_e), the Zone of Established Flow (ZEF) begins. Within this zone the velocity and concentration profiles become Gaussian. As a result, the time-averaged profiles of velocity or concentration can be expressed as a

maximum value at the jet centerline, and the distance from the jet centerline. The resulting formula for the velocity distribution takes the form of:

$$u = u_c \exp[-(z/b)^2] . \tag{2.7}$$

Where u_c is the centerline (maximum) velocity, x is the distance from the centerline, and b is the characteristic width of the profile. For a pure jet a characteristic length may be defined :

$$l_Q = \frac{Q}{M^{0.5}} \tag{2.8}$$

Expressions for the centerline velocity and momentum flux as functions of distance from the jet exit, z, can be derived (Fischer et al., 1979), as can expressions for the characteristic width, b:

$$u_c \frac{Q}{M} = 7.0 \frac{l_Q}{z} \tag{2.9}$$

$$\frac{\mu}{Q} = 0.25 \frac{z}{l_Q} \tag{2.10}$$

$$\frac{b_w}{z} = 0.107 \tag{2.11}$$

$$\frac{b_t}{z} = 0.127 \tag{2.12}$$

Where b_w = the characteristic width of the velocity profile (Gaussian).

b_t = the characteristic width of the concentration or temperature profile.

Provided that $z >> l_Q$.

In a similar fashion, it is also possible to define the centerline concentration as a function of z, and the concentration with distance from the centerline:

$$C_m/C_o = 5.64(l_Q/z) \tag{2.13}$$

$$C = C_m \exp\left[-\left(x/b_t\right)^2\right] \tag{2.14}$$

As a consequence of the shear between the jet and ambient fluid, entrainment of ambient fluid into the jet will occur. In formulating an approach to the entrainment problem, Morton et al. (1956), proposed that the velocity of the inflowing diluting fluid be proportional to the local centerline velocity of the jet. The resulting expression for the entrainment flux was $Q_e = 2\pi\alpha b u_c$, where α is an entrainment coefficient. Further research (List and Imberger, 1973) revealed that α was not a constant, but in fact was a function of the local densimetric Froude number.

An alternate approach, and one that is more easily applied, is to assume a constant spreading angle for the jet, as proposed by Abraham (1965). With this approach the diffusion layer is assumed to spread linearly. It has been shown that the spreading angle, $db/dz = \varepsilon$, varies by less than 10% between the extreme end cases of pure plumes and jets, while α varies widely with F_o. Jirka (1975) further demonstrated that the two approaches were consistent, and ε could be related to α for both the case of a jet or plume.

2. 1. 2.   Pure Plumes

For a pure plume, both the initial momentum and volume fluxes are zero. An expression for the center line vertical velocity in a plume is:

$$u_c = 4.7\frac{B^{1/3}}{z^{1/3}} \tag{2.15}$$

As the plume rises the momentum flux increases from its initial value of zero to:

$$\mu = 0.254 m^{1/2} z \tag{2.16}$$

2. 1. 3.   Buoyant Jets

Buoyant jets are hybrids of jets and plumes, the fluid being discharged is buoyant, but also has significant initial momentum. In addition to the length scale l_Q, used to

characterize pure jets, an additional characteristic length scale is introduced for buoyant jets:

$$l_M = \frac{M^{3/4}}{B^{1/2}}$$
(2. 17)

The ratio of l_Q to l_M is the initial jet Richardson number:

$$R_o = \frac{l_Q}{l_M} = \frac{QB^{1/2}}{M^{5/4}}$$
(2. 18)

When the initial jet Richardson number, R_o, approaches a critical value, the plume Richardson number ($R_p = 0.557$), then the buoyant jet actually behaves as if it were a pure plume right from its origin. In a manner similar to that for pure jets, Fischer et al. (1979), presents expressions for the dilution of a buoyant jet, where:

$$\overline{\mu} = \frac{\mu}{Q}\left(\frac{R_o}{R_p}\right)$$
(2. 19)

$$\varsigma = c_p\left(\frac{z}{l_Q}\right)\left(\frac{R_o}{R_p}\right)$$
(2. 20)

Where $c_p = 0. 254$, and the volume flux then becomes:

$$\overline{\mu} = \varsigma \qquad\qquad \varsigma << 1$$
(2. 21)

$$\overline{\mu} = \varsigma^{5/3} \qquad\qquad \varsigma >> 1$$
(2. 22)

It is interesting to note that all buoyant jets will eventually become plumes, once they have traveled a great enough distance. The determining parameter for whether a buoyant jet will behave as a plume, or as a jet, is the ratio of z to l_M . If $z >> l_M$ then the buoyant jet will behave as a plume, conversely if $z << l_M$ then the buoyant jet will retain its jet like behaviour. Therefore, if l_Q and l_M are of the same order, the buoyant jet will become plume like in behaviour very close to the jet exit.

2. 2. Buoyant Jets In Shallow Water

2. 2. 1.   Water Depth Classification

There are a number of different schemes for classifying water depth when dealing with jets and plumes, with each researcher apparently using a different one. For the purposes of this review a uniform classification of water depth will be applied. Under this scheme water depths will be divided into four categories, each category being defined by the characteristics of a jet discharged into it (Refer to Figure 2.2). The four categories of depths that will be employed are: deep water, shallow water, very shallow water, and extremely shallow water. These categories are defined as follows:

Deep Water

Generally speaking, deep water can be defined as water with a depth above the outlet much greater than 20 port diameters ($h_1/D \gg 20$). Velocity and density profiles of the vertical jet can be treated as self-similar or Gaussian. Should the jet reach the surface, no significant surface disturbance can be expected. If the water is sufficiently deep, $H \gg l_Q$, then a buoyant jet will develop into a plume and buoyancy effects will be dominant.

Shallow Water

Within shallow water, velocity and density profiles of the jet outside the zone of flow establishment may still be treated as Gaussian. However a surface disturbance and surface spreading layer may be expected. If the jet does not have sufficient buoyancy or has high momentum flux then there is a possibility of a recirculating or unstable flow. Based on the definition of Lee & Jirka (1981), shallow water depths are from 6 to 20 port diameters ($6 < h_1/D \le 20$).

Very Shallow Water

For jets with $F_o > 25$ the length of the Zone of Flow Establishment (ZFE), z_t, is approximately $6D$. As F_o decreases below approximately 8, the length of the ZFE

decreases quickly to a minimum of $2D$ for F_o of approximately 1 (refer to Figure 2.3). Since for most practical cases the densimetric Froude number will be greater than 8, z_t can be assumed to be approximately $6D$. When $z < 6D$, there exists a jet core in which the velocity remains at the jet exit velocity, and turbulent shear forces have not penetrated into the jet. As a result, in the ZFE, Gaussian velocity and density profiles are not appropriate. Also, the thickness of the surface impingement region may be a significant proportion of the water depth over the discharge. Based on this, the range for very shallow water is defined as 2 to 6 port diameters $(2 < h_1/D < 6)$.

Extremely Shallow Water

Crow and Champagne (1971) demonstrated that the entrainment flux for a jet is constant, and that a "top-hat" velocity profile was appropriate for water depths of less than 2 port diameters $(h_1/D \leq 2)$. From this, extremely shallow water is defined as having a depth less than 2 port diameters $(h_1/D \leq 2)$.

2. 2. 2.   Buoyant Jets In Shallow Water

The study by Lee & Jirka (1981) on shallow water jets has formed the basis for later work by many researchers. As part of their study, Lee & Jirka (1981) examined shallow water jets over a wide range of flow conditions. Experimental studies were carried out on semicircular vertical buoyant wall jets with densimetric Froude numbers $(F_o = U/(g'D)^{1/2})$ ranging from 8 to 583. Depths used in the study were between 6 and 35 port diameters, and jet Reynolds numbers were sufficiently high for all runs to ensure fully turbulent conditions. In developing their model of shallow water jets, Lee & Jirka (1981) divide the flow into four regions (described below): buoyant vertical jet region, surface impingement regions, radial internal hydraulic jump, and stratified counterflow region. The first three regions comprise the near field (momentum dominated), and the last region makes up the far field (buoyancy dominated). See Figure 2.4.

Buoyant Vertical Jet Region

In this region the vertical buoyant jet entrains ambient fluid as it moves toward the surface. Where the jet enters the surface impingement region, the velocity and density profiles are assumed to have become self similar or Gaussian, since Lee & Jirka (1981) assume depths greater than six port diameters.

Surface Impingement Region.

Within this region, the vertical flow of the buoyant jet is redirected to a horizontal radially spreading flow. A surface boil, or fountain, is associated with this region. There is assumed to be intense turbulent mixing, but no entrainment, within this region. It is assumed that little or no entrainment occurs in this region, since the surface impingement region is bounded almost completely by the vertical buoyant jet and radial internal hydraulic jump region. The surface impingment region has almost no interfacial area with the ambient fluid. At the point where the flow exits from the surface impingement region, the velocity profile is assumed to be half-Gaussian.

Radial Internal Hydraulic Jump Region

The flow is transformed from a supercritical surface flow to a subcritical flow by passing through an internal hydraulic jump. There is an abrupt increase in upper layer thickness, and an energy loss, associated with the radial internal hydraulic jump. Based on theory for two-layer flows, Lee & Jirka (1981) were able to develop expressions for estimating the conjugate layer depths upstream and downstream of the internal hydraulic jump. This region will exist when the jet discharge is considered stable. That is, when the discharged fluid has sufficient buoyancy to form a surface layer upon exit from the surface impingment zone, and to prevent being re-circulated and re-entrained into the jet. If the momentum of the jet were high relative to the buoyancy of the jet, an unstable flow configuration would exist. As will be discussed later, there is some dispute over the

existence of an internal hydraulic jump in this transition from near-field to far-field conditions.

Stratified Counterflow Region

This region is made up of the buoyant upper layer flowing outward from the source and the denser ambient fluid of the lower layer flowing inward to the vertical buoyant jet. Velocities are relatively low, and entrainment across the interface of the two layers is considered negligible.

An unstable configuration is one in which the buoyancy of the discharged fluid is not sufficient to cause the flow to form a distinct, stable upper layer. The downward momentum of the fluid exiting the surface impingment zone, combined with the shear between the outward flowing upper layer and the inward flowing ambient fluid in the lower layer, causes the upper layer to fill the entire depth of the near-field, and re-circulation and re-entrainment into the jet fluid occurs. In an unstable configuration, a distinct surface layer only forms in the Stratified Counterflow Region. This flow configuration is not considered desirable as it has the effect of reducing dilution.

Lee & Jirka (1981) developed a criteria for stability of the near-field region. This criteria may be expressed as a function of the densimetric Froude number $(F_o = U/(g'_o D)^{1/2})$, and H/D. Refer to Figure 2.5. The flow configuration is considered stable when:

$$F_o < 4.6(H/D) \qquad \text{for } H/D > 6 \qquad (2.23)$$

Thus, when the densimetric Froude number is greater than a certain value determined by H/D, the flow will be unstable. If the source conditions (F_o, D) are fixed, then decreasing the depth H beyond a certain value will result in the flow becoming unstable.

Central to Lee & Jirka's approach to the problem of vertical buoyant jets in shallow water, is the assumption that the transition from near-field to far-field conditions is accomplished by means of an internal hydraulic jump. This assumption is disputed by

other researchers, as will be discussed below. Lee & Jirka (1981) do not present any velocity measurements to verify that there are conditions of internally supercritical and internally subcritical flow upstream and downstream of the supposed location of the internal hydraulic jump, to support their contention that this is a valid approach. It is possible that the presence of a downstream control in Lee & Jirka's experimental work may have created an internal hydraulic jump that would not otherwise have been present.

A further, modified development of Lee & Jirka's approach is presented in Wright et al. (1991). In this model, it was assumed that the radial surface flow results in greater dilution than that in the vertical buoyant jet alone, it was further assumed that entrainment does occur in the internal hydraulic jump, where as Lee & Jirka (1981) did not. In formulating their model, Wright et al. (1991) assumed that the flow exiting the internal hydraulic jump is internally critical. This contradicts the formal definition of an internal hydraulic jump in which the flow must be internally supercritical upstream of the jump, and internally subcritical downstream and is probably incorrect. However, this assumption has the advantage of allowing the equations of Wright et al.'s model to be more easily solved, since the form and degree of downstream control could be ignored, and was probably adopted for this reason. It is not clear whether this is actually valid for the real situation or is merely an expedient measure. It was noted that the model was most sensitive to the assumed length of the internal hydraulic jump.

Wright et al (1991) also presented a stability criteria, the flow configuration was unstable, and re-circulation of the upper layer back into the vertical jet would occur when:

$$\frac{l_M}{H} > 6 \qquad\qquad (2.24)$$

By substituting for l_M, and rearranging equation 2.24, the following is obtained:

$$F_o = 7.63\left(\frac{H}{D}\right) \qquad\qquad (2.25)$$

This result for the stability criterion has the same form as that of Lee & Jirka (1981). Since Wright et al. (1991) noted that the coefficient on the right hand side of equation 2.23 could vary between 3 and 6, with the result that the coefficient in Equation 2.24 could vary between 3.8 and 7.63, this indicates that these results are in relatively close agreement with those of Lee & Jirka.

2. 2. 3.   Surface Impingement and Disturbance

If the ambient water is sufficiently shallow, then the jet momentum will still be concentrated into a relatively small jet core, and will not have been spread out by entrainment. As the buoyant jet impinges on the free surface, a surface disturbance or boil is created. This surface boil produces a radial pressure gradient which redirects the flow from a vertical jet into a radial horizontal flow. The radius of the region of surface impingement is defined as corresponding to the radius in the vertical jet at which the velocity, u, is 5% of the centerline (maximum) value, u_c, at the point of entry to the surface impingement region. At the exit from the surface impingement region most researchers assume that the radial velocity profiles are half-Gaussian. Lee & Jirka (1981) present diagrams for determining the thickness of the surface impingement region as functions of F_o and H/D (Refer to Figure 2.6).

It is possible to estimate the maximum height of the surface disturbance. Making use of the results of Murota & Muraoka (1967), Labridis (1989) provided an expression for the maximum height of the surface disturbance:

$$h_B = 1.61 \frac{D^{7/4}}{H^{3/4}} F^{3/2}$$

(2.26)

Many researchers including Murota & Muraoka (1967), and Labridis (1989), have noted that the surface disturbance does not approach the ambient water surface monotonically, but that a small ring around the boil is depressed below the level of the ambient water. This result is particularly noted as the ambient water becomes increasingly

shallow. It is believed that this occurs because the water which flows up to the top of the hump then develops downward momentum as it flows outward horizontally from the crest of the hump.

Due to the complexity of the flow structure within the surface disturbance, it would be difficult to analytically describe the flow within the surface impingement region. As a result, most researchers have relied upon a control volume approach, and simplifying assumptions, such as half-Gaussian velocity profiles at the exit from the region, e.g. Lee & Jirka (1981) and Labridis (1989).

2. 2. 4.   Additional Effects of Shallow Water

Lee & Jirka (1981) presented a graph that shows that for $F_o < 10$, the non-dimensionalized length of the ZFE, $Z_t = (z_t/D)$, varies considerably with F_o. For $F_o > 25$, Z_t asymptotically approaches a value of approximately 5.74, (Refer again to Fig 2.3). Thus for many practical situations, when the ambient water depth (H) is less than six port diameters, the jet flow will not reach a state of established flow, and velocity and density profiles will not be Gaussian. Some researchers (Labridis (1989)) define water depths where $H \leq 6D$ as very shallow water because of this situation.

Crow & Champagne (1971) studied non-fully developed jets, and determined that for $h_1/D < 2$ and $H/D < 6$ the following equations applied for Q and M, at the boundary (section 1) between the vertical jet and the surface impingement zone:

$$Q_1 = Q_o(1 + 0.136h_1/D)$$

(2.27)

$$M_1 = M_o(1 + 0.136h_1/D)$$

(2.28)

It has also been reported (Murota & Muraoka (1967)), that for $H < 20D$, that the spreading angle of the jet within the Zone of Flow Establishment is greater than that for a free jet. This could be due to the formation of helical vortices around the jet. The unbalanced forces produced by the helical vortiex on alternating sides of the jet would

cause the jet to oscillate about its centerline. This would make the jet appear wider than it actually was as it oscillates through its range of movement.

Labridis (1989) demonstrated that for $z_e \ll l_M$, the jet Froude number $(F = U/(gD)^{1/2})$ will be of more significance than F_o, since when $z_e \ll l_M$ the momentum of the jet dominates the flow and the jet's buoyancy is relatively unimportant. This implies that for shallow and very shallow water F will be more important than F_o, since $z_e \ll l_M$. As a result, Labridis re-expressed the stability diagram of Lee & Jirka in terms of F instead of F_o, refer to Fig 2.7. The stability criteria of Lee & Jirka (1981) re-expressed in terms of F by Labridis (1989) is:

$$F = 0.32(H/D) \qquad (2.29)$$

2. 2. 5. Buoyant Jets In Extremely Shallow Water

Lawrence & Bratkovitch (1993) developed an alternate approach for the behaviour of a vertical buoyant jet discharged into extremely shallow water ($H/D < 2$ and $h_1/D < 2$). Because of the extremely shallow depths, an assumption of Gaussian velocity and density profiles in the vertical jet was inappropriate. Instead, the results of Crow & Champagne (1971) were made use of, and "top-hat" velocity profiles were assumed in the vertical buoyant jet. This also allowed the assumption of constant entrainment flux in this portion of the jet. The situation involving jets in very shallow water ($6 < H/D > 2$, and $6 < h_1/D < 2$) was not dealt with, as the behaviour of a jet under these conditions is not well understood, representing as it does a transition from the ZFE to ZEF conditions in the jet.

The Lawrence & Bratkovitch (1993) model is broken up into four regions in a manner similar to that employed by Lee & Jirka (1981), but there are some important differences. The four regions in the Lawrence & Bratkovitch (1993) model are; vertical buoyant jet; surface impingement zone; radial buoyant jet; and radial buoyant plume (Refer to Figure 2. 8). The chief difference between the Lawrence & Bratkovitch (1993) model

and the Lee & Jirka (1981) model lies in the assumption made by Lee & Jirka (1981) that the transition from near-field to far-field (radial buoyant jet to radial buoyant plume) is accomplished by means of an internal hydraulic jump. Lawrence & Bratkovitch (1993) argue that the radial buoyant jet entrains ambient fluid until buoyancy causes entrainment to cease, and the radial buoyant jet becomes the radial buoyant plume in the far field. Lawrence & Bratkovitch dispute the existence of an internal hydraulic jump as the mechanism of transition between near-field and far-field, as a downstream control would be required to induce the internal hydraulic jump, and in the absence of a downstream control such a jump would not form. The mechanism by which transition from near-field to far-field may occur will be discussed further below.

In addition to the assumption of "top-hat" velocity profiles in the vertical buoyant jet region, the Lawrence & Bratkovitch (1993) model makes use of the following assumptions:

- Constant momentum flux in the vertical buoyant jet, radial buoyant jet, and radial buoyant plume. The existence of energy and momentum loss in the surface impingement region was recognized, but was considered negligible based on Lee & Jirka's result that their solution was not sensitive to energy loss.

- Constant buoyancy flux in near field, with buoyancy flux decreasing in far-field over time due to assumed heat loss. In modeling the decrease in buoyancy due to heat loss from the radial buoyant plume, it was assumed that density varies linearly with temperature. For warm discharges, the assumption that density varies linearly with temperature is reasonable, since the relationship between temperature and density is approximately linear above 15°C. In the far-field, where dilution and heat loss to the atmosphere will lead to significantly decreased temperatures, and a non-linear temperature-density relationship, this would not be valid and would be subject to greater error.

Lawrence & Bratkovitch developed the following equations for conditions at section 1, the entrance of the vertical buoyant jet to the surface impingement region:

$$\frac{Q_1}{Q_o} = \frac{r_1}{r_o} = \frac{u_o}{u_1} = \frac{g_o{}'}{g_1{}'} = 1 + 0.065\frac{h_1}{r_o} \qquad (2.30)$$

Provided that $h_1/r_o \le 4\,(h_1/D \le 2)$.

In the surface impingement region negligible entrainment was assumed by Lawrence & Bratkovitch (1993), and therefore at section 2, the exit from the surface impingement region to the radial buoyant jet region, $Q_2 = Q_1$ and $g'_2 = g'_1$. Lawrence & Bratkovitch (1993) followed Lee & Jirka (1981), in assuming that section 2 occurs at the radius, r_2, at which the velocity in the vertical buoyant jet falls to 5% of its centerline value at section 1. As a result of this assumption, and making use of equation (2.30), Lawrence & Bratkovitch obtained:

$$r_2 = r_o\left(1 + 0.125 h_1/r_o\right) \qquad (2.31)$$

Again provided that $h_1/r_o \le 4\,(h_1/D \le 2)$.

Based on this result, and in applying conservation of mechanical energy in the surface impingement region, Lawrence & Bratkovitch (1993) then predicted that the thickness of the surface impingement region was nearly constant for the range $0 \le h_1/r_o \le 4$ with $h_2/r_o = 0.5$.

Within the radial buoyant jet region, Lawrence & Bratkovitch (1993) reason that shear instabilities as a result of the radial flow of the buoyant jet over the counter flowing ambient fluid cause further entrainment and the upper layer will grow in thickness. The growth rate of the radial buoyant jet was modeled as:

$$\frac{dh}{dr} = \alpha v_r\, f(Ri) \qquad (2.32)$$

Where: $\quad \alpha = $ growth rate coefficient.

$$v_r = \frac{\overline{U} - \overline{U}_{ret}}{\left(\overline{U} + \overline{U}_{ret}\right)}, \text{ velocity ratio.}$$

$\overline{U}_{ret} = $ the depth averaged return flow in the lower layer.

$$\overline{U} = \text{the depth averaged flow in the upper layer.}$$

$$\text{Ri} = \frac{g'h}{\Delta U^2}, \text{the bulk Richardson number.}$$

$$\Delta U = \overline{U} - \overline{U}_{ret}$$

The bulk Richardson number contained in equation 2.32 is important to Lawrence & Bratkovitch's (1993) model. Initially, the bulk Richardson number will be less than a certain critical Richardson number, Ri_c. While this is the case, shear instabilities will entrain ambient fluid into the radial buoyant jet, increasing its thickness until Ri_c is reached, and buoyant forces stabilize the flow, and entrainment ceases.

If the bulk Richardson number does not approach its critical value, and the velocity ratio, v_r, instead approaches infinity, then the flow will become unstable. The velocity ratio will approach infinity when the velocities in the upper and lower layers are of approximately equal magnitudes, though in opposite directions. This will occur when the water is too shallow and/or the jet has a very high volume flux.

If the flow is stable in nature then the transition from near-field to far-field occurs at the point where the critical Richardson number, Ri_c, is reached. Lawrence & Bratkovitch (1993) made use of the results of Chen (1980) in determining the growth rate of the radial buoyant jet. In working with Chen's data the best fit was found for $\alpha = 0.08$ and $f(\text{Ri}) = 1 - \text{Ri}/\text{Ri}_c$. In addition, Ri_c was found to be approximately 0.3. Others have suggested that α should be in the range of 0.015 and that a different form of $f(R_i)$ should be employed. However, $\alpha = 0.08$ is close to the values found for circular plumes.

The composite Froude number is defined as follows:

$$G = \frac{\overline{U}^2}{g'h_u} + \frac{\overline{U}_{ret}^2}{g'(H - h_u)} \tag{2.33}$$

The composite Froude number indicates whether the flow is internally supercritical, internally critical, or internally subcritical. The significance of the composite Froude number, is that when the flow is internally supercritical or internally critical, long

internal waves can not propogate upstream against the flow. Thus, under internally supercritical or internally critical conditions the effects of internal hydraulic jumps, or other similar features, cannot propagate upstream.

If constant momentum flux in the far-field is assumed, then sample calculations using equation 2.32 (refer to section 3.1) reveal that the composite Froude number, G, approaches 1 asymptotically. This result is essentially the same as the assumption of internally critical flow in the distant far-field made by Wright et al. (1991), in developing their model. According to Wright et al. (1991), these conditions imply that the internal hydraulic jump is of the maximum entraining type, and shear layer growth is maximized.

2. 2. 6.   Mechanisms of Near-Field to Far-Field Transition

There are two contrasting approaches to the treatment of the transition of the radial buoyant surface jet from near-field to far-field conditions. Generally, most researchers have followed the approach of Lee & Jirka (1981) in assuming that a radial internal hydraulic jump exists. Others have argued that this is only valid under certain conditions, namely an imposed downstream control, which would induce an internal hydraulic jump. The most important of these is Wood & Wilkinson (1971).

2. 2. 6. 1. Entrainment Layer Approach

Wilkinson & Wood (1971) examined the occurrence of an internal hydraulic jump, or density jump, for a dense liquid discharged at the bottom of a channel. Two major regions were identified in a density jump (Refer to Figure 2.9). In the first of these, the entrainment region, there exists interfacial shear which gives rise to interfacial instabilities, and therefore entrainment. Downstream from the entrainment, region a roller region may occur depending on downstream conditions. In the roller region there is a reverse flow near the interface with the ambient fluid, and interfacial shear is considerably lower. Entrainment in the roller region is negligible. It is important to note the definition of a density jump as employed by Wilkinson & Wood (1971). In their scheme, a density jump

is composed of either an entrainment zone, or internal hydraulic jump, or possibly both, depending upon flow conditions. Since an internal hydraulic jump is not necessarily present, the term density jump may be misleading, it may not resemble a "jump" at all.

Of importance is Wilkinson & Wood's observations of the behaviour of the internal hydraulic jump as downstream control is varied. In order for a roller region to exist, Wilkinson & Wood (1971) determined that it was necessary for a downstream control such as a weir, or channel constriction, to exist. The greater the control that was exerted, the less the extent of the entrainment region, with the roller region being pushed farther upstream. If the downstream control, such as weir height, were increased beyond a certain point, it was found that the entrainment zone ceased to exist, any further increase in the control exerted would then result in the density jump becoming flooded. As the degree of downstream control was reduced, the greater became the extent of the entrainment region, until finally, with little or no downstream control, the entrainment zone occupied the complete length of the density jump, and the roller region had died out. In short, in the absence of a downstream control, only an extended entrainment region featuring interfacial instabilities due to shear existed.

Lawrence (1985) investigated the occurrence of internal hydraulic jumps, and associated mixing, in two layer flow in a channel. The flume used in these experiments was 12.8 m long by 0.38 m wide. When the flume was free from obstacles, the flow lacked an internal hydraulic jump, and there was no significant entrainment occurring. Internal hydraulic jumps were only present when a stationary obstacle, in the form of a sill, was introduced to the channel. The internal hydraulic jump would form downstream of the obstacle. Often shear instabilities, of the Kelvin-Helmholtz variety, were observed in the approach to the internal hydraulic jumps. These instabilities resulted in entrainment of fluid occurring at the density interface. Of most importance though, is the observation that internal hydraulic jumps would only occur when an obstacle was placed in the

channel. Even though the channel was very long, friction from the bed and sides of the channel was insufficient to cause the occurrence of an internal hydraulic jump.

Koop & Browand (1979) investigated the entrainment and mixing which occurred at a density interface in a two layer flow in a long channel. In their experiments both layers were flowing in the same direction, though at different velocities. As for Lawrence (1985), they did not observe the presence of an internal hydraulic jump in the channel. Instead, interfacial instabilities, in the form of vortices, initiated at the entrance to the channel. As these vortices moved down the channel they grew in size, and merged. At some point in the channel the instabilities would reach a maximum size. When this occurred the instabilities would collapse into a stable interface, with only small instabilities present, the turbulence generated by these large scale instabilities having been dissipated. Koop & Browand (1979) reason that the large scale structures are critical in the formation and maintenance of turbulence. The statically stable conditions arising from the density difference results in the ultimate destruction of the turbulence generated. Koop & Browand (1979) provide an explanation as to why the collapse of the vortex structures occurs. As a vortex grows, it lifts denser fluid, and depresses lighter fluid into the lower layer. As vortex size increases, it requires greater energy to accomplish this, eventually there will be insufficient energy, and the turbulent structure collapses.

In studying the discharge of a horizontal surface buoyant jet, Koh (1971), observed the existence of an entrainment region immediately after the jet exit. In this region ambient fluid is entrained into the surface jet, which grows in thickness. The end of this region marks the transition from near-field to far-field. In a manner similar to Lawrence & Bratkovitch (1993), this transition was modeled as occurring when the Richardson number of the flow reached a critical value, and the turbulent entrainment collapsed under the influence of buoyancy.

Similar results were reported by Chen (1980). Experiments with a radial surface buoyant jet in a circular tank produced a region of flow with increasing thickness, and

entrainment occurring, until at a distance equal to the length scale defined by M and B (l_M), the entrainment structure collapsed, and the radial jet became a radial plume. From this point outward, until the spreading radial plume contacted the walls of the experimental tank, the radial plume was of constant depth. It is interesting to note that Chen (1980) also observed that once the jet had contacted the walls, the surface layer increased in thickness due to the flow being choked off. This resulted in the entrainment zone being "drowned" and an internal hydraulic jump forming.

2. 2. 6. 2.   Internal Hydraulic Jump Approach

In contrast to the evidence presented above, which argues the existence of an entrainment zone in the absence of a downstream internal control, rather than an internal hydraulic jump, is the conflicting position taken by some researchers which promotes the internal hydraulic jump argument. Andreopoulos et al. (1986) and Wright et al. (1991) both state that an internal hydraulic jump should be present, though the results of their own experiments contradict them.

In experiments designed to investigate the effect of an imposed downstream control on a vertical plane buoyant jet discharged in shallow water, Andreopoulos et al. (1986) (inadvertently) largely confirmed the results of Wood and Wilkinson (1971). In the absence of an imposed downstream control, in this case a submerged weir, no roller region was observed, and only an entrainment region was present. Within the test channel, entrainment was observed to cease as buoyancy stabilized the flow downstream. In spite of the apparent absence of the roller region, Andreopoulos et al. (1986) still term this an internal hydraulic jump. Andreopoulos et al. (1986) further argue that the downstream control would have been provided by channel and/or interfacial friction, had their experimental channel been long enough.

The reasoning employed by Andreopoulos et al. (1986), that channel friction would be sufficient to force an internal hydraulic jump, does not appear to be supportable.

Wood and Wilkinson (1971) were explicit in their results from experiments in a long channel. An internal hydraulic jump with roller region was only present when a strong internal control, such as a hump or contraction, was placed in the channel. If channel and interfacial friction were likely to produce an internal hydraulic jump, it would have been most evident in Wood & Wilkinson's experiments. In their experimental configuration, the higher speed flow was in the dense layer located at the bottom, against the solid floor of the channel, friction would have been greatest in this situation. Yet an internal hydraulic jump was not created without a channel control. In the experiments conducted by Andreopoulos et al. (1986) the fast flowing layer was the less dense one at the top, farthest from the channel bottom, and hence channel friction was likely less than that of Wood & Wilkinson (1971). No internal hydraulic jump was observed until Andreopoulos at al. (1986) introduced a sill into the upper layer.

Andreopoulos et al. (1986), provide further theory into the behaviour of the jet discharge in the absence of the downstream control. Andreopoulos et al. (1986) states:

> "The surface jet flow is supercritical, i. e. the densimetric Froude number
> based on the local layer thickness, velocity, and density difference to the
> ambient is larger than 1"

This is not a valid concept, since whether the surface flow itself is supercritical or not would depend on the regular Froude number, not on the densimetric Froude number. If the two layer flow itself is being referred to, then the quantity of importance for determining whether the flow is internally supercritical or not is the composite Froude number, G, discussed previously. Andreopoulos et al. (1986) then go on to state that as entrainment occurs the Froude number is reduced until a locally critical flow condition is achieved (F=1). This is in contrast to Wright et al (1991), who state that for a radial flow, the downstream flow is internally critical, e. g. $F_1^2 + F_2^2 = 1$ as opposed to $F_1^2 = 1$. Andreopoulos et al. (1986) also note that when a roller is present the upstream flow is locally (externally) supercritical, and the downstream flow is locally (externally) subcritical, as would be expected for a "genuine" hydraulic jump.

As stated previously, Wright et al. (1991) assumed that the downstream (far-field) flow would be internally critical, since this would allow a steady state condition to exist without the need to specify downstream conditions. If the flow is internally critical, this would have the effect of blocking internal long waves, and therefore negate the effect of any downstream control. However, it is not stated what conditions would be necessary to ensure internally critical flow in the far-field, or whether this would actually occur in practice. This condition was also implicitly assumed by Lawrence & Bratkovitch (1993) in the structure of their model, as the flow moves outward radially, G^2 approaches 1 asymptotically. Thus, the flow approaches the internally critical condition as it spreads from the surface impingement zone.

Wright et al. (1991) formulate their model based on the presence of an internal hydraulic jump in at least a portion of the near-field region. Yet, further evidence supporting the existence of an entrainment region and interfacial instabilities, as opposed to an internal hydraulic jump, is provided by Wright et al. (1991) themselves. Wright et al. (1991) conducted laboratory experiments to validate their model. Two different experiments, one with a negatively buoyant jet, and the other with a positively buoyant jet discharged upward, were conducted. Only written descriptions are provided of the resulting flows, with the exception of two photographs. Wright et al. (1991) refer to the occurrence of ring vortices propagating outward from the jet location. These vortices appeared to extend through the whole depth of the upper layer, and may be a form of shear instability. At the same time, no roller region was observed, indicating that the process does not involve an internal hydraulic jump. Closer to the jet, smaller scale turbulent fluctuations were observed, these tended to die out with increasing distance from the point where the jet was discharged. Finally only the large scale fluctuations, the ring vortices, remained, at the transition to far-field conditions even the large scale fluctuations were observed to die out. This is analagous to the results provided by Koop & Browand (1979).

Vortex ring structures were reported by Garvine (1984) in a radially spreading surface buoyant jet where a river flowed into ocean water. Observations of vortex ring structures in other surface buoyant plumes undergoing radial spreading were also made by Scarpace & Green (1973), and McClimans (1978). Laboratory investigations by Alavian & Hoopes (1982) have also revealed vortex ring structures. Rottman & Simpson (1983) also observed vortex rings in the radially spreading regions of a negatively buoyant jet discharged vertically downward to a surface.

2. 2. 6. 3.   Summary of Approaches to Transition Mechanisms

To summarize, many researchers have reported results supporting the existence of an entrainment region in the near-field, leading into the stable, stratified far-field. The existence of large scale instabilities, in the form of vortices, has been reported in both the cases of two layer flow in a channel, and for radial spreading flow from a vertical jet in shallow water. Internal hydraulic jumps have only been reported when an obstacle of sufficient size to act as an internal control has been placed in the flow. In spite of this evidence, some researchers continue to maintain that the transition from near-field to far-field conditions will occur by way of an internal hydraulic jump. This appears to be based on an intuitive belief that a radial internal hydraulic jump will be produced by interfacial friction, though experimental results do not support this. The convenience of solving mathematical equations formulated using the assumption of an internal hydraulic jump may also help to perpetuate this position.

Interfacial or channel friction has been cited as justifying the use of an internal hydraulic jump in models. However, as discussed previously, investigations of two layer flow in channels has shown that friction effects do not produce internal hydraulic jumps. Friction is even less likely to produce an internal hydraulic jump in stratified radial flows. As the radial distance increases, the velocities in the flows, and hence the friction, whether interfacial or boundary, decreases. Also, radial flows are not subject to sidewall friction.

This is in contrast to channel flow, where constant width, and therefore constant velocities, are maintained throughout the channel, and friction against the sidewalls is present.

Chapter 3

Experiments

3. 1. Prediction of Flow Conditions

In order to design the experiments undertaken in this study, it was considered desirable to attempt to predict the behaviour of the radially spreading flow in the proposed experimental apparatus. In order to make these predictions, it was necessary to make use of one of the models mentioned in the previous chapter. The best available model for predicting the radially spreading flow was that of Lawrence and Bratkovitch (1993). This model has not been confirmed experimentally and is likely somewhat coarse, but does provide estimates necessary in designing the experiments. Basic jet relationships, as described in Fischer et al. (1979), were used to estimate the flow conditions in the vertical jet. These predictions were necessary in order to estimate the variation of the composite Froude number, G, of the two layer flow, and the Reynolds' number of the upper layer. These quantities are important for determining, respectively, whether the flow is internally supercritical, internally critical, or internally subcritical, and whether the upper layer flow is turbulent.

First the flow conditions and the resulting entrainment into the vertical jet had to be estimated. In order to determine the entrainment length, the thickness of the surface blocking layer was estimated using Figure 2.6, from Lee & Jirka (1981). This provides the depth of the surface blocking layer as a function of the depth ratio, H/D, and the densimetric Froude number of the discharge, F_0. Subtracting the surface blocking layer thickness from the available depth gave the length of vertical jet available for entrainment (z). Using this length, the flow entrained was calculated by using equation (2.10). This equation is not entirely applicable for the depth range over which it was used, equation

(2.10) being intended for z/D >>6, but it should provide a reasonable estimate of the flow entering the surface blocking region.

The radius of the boundary of the surface blocking region, r_1, was estimated by assuming that it would occur at the point where the vertical time-averaged velocity of the entering vertical jet had dropped to 5% of its centerline value (Refer to Figure 3.10 for definition sketch). This assumption has also been used by Lee & Jirka (1981), Wright et al. (1991) and Lawrence & Bratkovitch (1993), and it is employed for convenience. Most of the volume flux of the vertical jet is contained within this radius (95%) and vertical velocoties have diminished to relatively low values beyond it. This radius was calculated by equation (2.7). The flow exiting the surface blocking region was assumed to be completely mixed, due to the highly turbulent nature of the surface impingement zone, and it was assumed that no entrainment occurs within the surface blocking region.

The radially spreading flow was treated as having uniform ("top hat") velocity and density profiles to simplify computations. Stepwise calculations were made to determine the flow, upper and lower layer depths, and upper layer growth rate, at a series of discrete sections as a crude numerical solution. The growth rate of the surface layer was calculated using equation (2.31). The resulting flow at each section was calculated using conservation of momentum flux. As a result at each section, i:

$$\mu_i = Q_i = (2\pi r_i h_{u_i} M)^{1/2} \qquad (3.34)$$

Where: r_i = Radius at section i.

h_{u_i} = Depth of upper layer at section i.

The resulting flow in the lower layer at each section, i, due to entrainment, is:

$$Q_{e_i} = Q_i - Q_o \qquad (3.35)$$

The flow velocities at each section in the upper and lower layers are, respectively:

$$\overline{U} = Q_i / (2\pi h_{u_i} r_i) \qquad (3.36)$$

$$\overline{U}_{ret} = Q_{e_i} / \left(2\pi (H - h_{u_i}) r_i\right) \qquad (3.37)$$

Due to dilution the modified gravitational constant decreases as the flow progresses outward. This variation was assumed to be linear with temperature or concentration of dissolved solids, with the result that:

$$g'_i = g'_o \, Q/Q_i \qquad (3.38)$$

Using the above relationships, the bulk Richardson number could be calculated:

$$R_i = g' h_{ui} / \left(\overline{U} - \overline{U}_{ret} \right)^2 \qquad (3.39)$$

Then, using Equation 2.32, the rate of change of depth with radius (dh/dr) could be calculated. The depth of the upper layer could then be calculated for the next section by:

$$\Delta h_{u_i} = \left(\frac{dh}{dr} \right)_i \Delta r \qquad (3.40)$$

Based on the results of Koop & Browand (1979) and Chen (1980), as discussed by Lawrence & Bratkovitch (1993), growth of the upper layer was assumed to cease, and a stable interface form, when the bulk Richardson number (R_i) reached 0.3. The entrainment into the upper layer in the far-field region was then calculated assuming a constant upper layer depth, and conservation of momentum flux. This has the result that in the far field the upper layer Reynolds' number varies inversely with the square root of the radius.

At any section in the radial flow, the Composite Froude number, and the Reynolds' number for flow in the upper layer, could be calculated:

$$G = \frac{\overline{U}^2}{g'_i \, h_{u_i}} + \frac{\overline{U}_{ret}^2}{g'_i \left(H - h_{u_i} \right)} \qquad (3.41)$$

$$R_u = \frac{Q_i/(2\pi r_i)}{\nu} \qquad (3.42)$$

Variation in Composite Froude number for the two layer flow, and Reynolds' number for the upper layer flow, was then predicted for the range of proposed flow conditions for the experiment. Sample plots of Composite Froude and Reynolds' numbers

against the radius, made non-dimensional by dividing by r_1, are presented in Figure 3.11 A & B. The Composite Froude number was found to start relatively high, and then decrease rapidly with radius, asymptotically approaching 1 for very large radii. Thus, the flow for all proposed experiments appears to remain internally supercritical for the entire range of the experimental tank (from 0 to 82 cm radius), if effects of the free surface control at the weir are neglected, discussed later.

Similarly, for the range of flows proposed for the experiment (refer to Section 3.2.2.), the Reynolds' number of the upper layer remains above the critical Reynolds' number for open channel flow of approximately 550 (Daugherty et al. 1954), well beyond (>30 cm) where the boundary of the experimental tank would occur (This should not be confused with the critical Reynold's number for a jet of approximately 4000). While the value of 550 represents the critical Reynold's number for parallel flow in a straight open channel, and is not directly applicable to a developing radial flow, it does provide a point of comparison for an order of magnitude analysis. Considering that the calculated upper layer Reynold's numbers in Figure 3.11B are in excess of 2000, and hence well above 550, this indicates that the flow will remain turbulent well into the far-field region in the radially spreading surface layer.

3. 2. Experimental Design and Procedure

3. 2. 1. Experimental Design

In order to experimentally investigate the entrainment mechanisms, and manner in which the near-field to far-field transition takes place, it was necessary to produce a radially spreading surface jet. The main emphasis of this investigation was on flow visualization of the radial regions of the jet, to determine the mixing and transition mechanisms in the near- and far-fields. There were four important factors which influenced the design, these are discussed more fully below, but briefly they were:

1. simulation of an infinite ambient to avoid internal control effects.

2. ensuring symmetry of the flow.

3. allowing undistorted viewing for flow visualization.

4. allowing for replenishment of the ambient to replace entrained fluid.

The most serious consideration was to ensure that the experiment was capable of simulating an infinite ambient, when in fact the apparatus was very limited in extent. This required that the design allow for the outflow of the jet flow and the entrained fluid in a manner which would not choke the flow, and cause the onset of a radial internal hydraulic jump, as discussed in Chapter 2. This suggested a form of weir which would allow the upper layer of fluid to spill out of the experimental tank, while still containing the ambient fluid. A free surface local control of the upper layer flow over the weir would exist, but an internal control would not be imposed.

The effect of the circular weir upon the upper layer would be in the form of a free surface control where the flow would accelerate over the weir, in the same manner as over a spillway or similar structure. The existence of the underlying layer would have no effect upon the flow over this weir, since it would be below the level of the weir. The circular wall would not act as an internal control, as ambient fluid supplied from the ring diffuser (discussed below) would be flowing inward, away from the wall. Thus, the circular wall, which represents an artificial constraint not found in prototype situations, does not act as an internal control since the flow of ambient fluid effectively originates "downstream" of this wall and does not encounter it.

Since the intent of the experiment was to study the radially flowing surface regions of the jet, the boundary of the tank had to be configured so that it would allow the flow to be symmetrical. This condition dictated that the tank be circular with the jet discharge in the center. In order to ensure the symmetry of the flow, the weir had to be carefully leveled, any significant deviation in the level of the weir would tend to bias the flow in one direction or another, destroying the desired symmetry.

The circular weir or wall leads to a difficulty, in that the curved surface of the wall will tend to distort any view through the wall of the flow. Also the fluid spilling over the top of the weir, and flowing down the sides, would have interfered with photography. To overcome these problems, a square tank was constructed to contain the circular experimental tank. This tank was filled with water to within 1 to 2 cm of the top of the circular weir. This had the effect of minimizing the distortion of the curved wall of the circular tank, by allowing photography to occur through the flat surface of the square tank, through water, and then into the circular tank. The square tank also served to contain the outflow from the circular tank, the water level in the square tank being controlled by valves on the outlet lines.

Because the circular tank was relatively small in volume, the available ambient fluid in the tank would have been quickly depleted, particularly at the higher discharge rates of the jet. Thus a scheme whereby the ambient would be continually recharged to replace lost fluid, and maintain steady state conditions, was designed. Using a cold water supply in the lab, a supply line was run through a control valve and flow meter, and then split into two lines, which were connected to two diffuser like discharge tubes in the bottom outside edge of the circular tank. These diffuser tubes were installed such that they discharged straight inwards toward the vertical jet, to approximate the gross flow of the ambient fluid toward the center to replace entrained fluid. In order to minimize mixing created by jets from the ring diffuser, synthetic air filter material was wrapped around the ring diffuser to baffle the flow, and diffuse the jets. Refer to Figure 3.12 for a schematic of the experimental apparatus, Figure 3.13 provides a photograph of the apparatus.

It was necessary to balance a number of considerations in developing the final design of the experimental tank and apparatus. The maximum flow rates were limited by the capacity of the water supplies in the lab. Most critical was the available hot water supply, which, from a 2.5 cm domestic line, was capable of supplying a maximum flow of from 2 to 2.5 l/s (30 to 37.5 USGPM) depending on other demands. Steady state water

temperature at full demand was approximately 50°C. Temperature of the cold water supply varied between 8°C and 10°C, with a maximum flow rate of approximately 6 l/s.

Minimum flow rates used in experiments were dictated by the requirement to ensure that the flow remained turbulent well into the far-field region, so that the mechanisms of interest were present. For the vertical jet region, this required that the Jet Reynolds' Number be greater than 4000. Prediction of the Reynolds' number of the radially spreading flow was discussed in the preceding section.

To investigate the effect of the ratio H/D, a series of jet nozzles of different diameters were fabricated. These nozzles were equipped with standard fittings for attachment to the circular tank and connection to the hot water line. Extensions to allow the effect of different h_1/D ratios to be investigated were also manufactured.

The dimensions of the circular tank were 30 cm deep with a diameter of 183 cm. The square containment tank was 213 cm by 213 cm by 34 cm deep. Both tanks were constructed from clear Plexiglas GM. The flow meter used on the jet discharge was a King Instrument Company variable area flow meter, model number K72-05-0465, for flow ranges from 0.1 l/s to 2.5 l/s (1.5 to 37.5 USGPM). The flow meter used on the ambient recharge was a King Instrument Company variable area flow meter, model number K72-05-0251, for flow ranges from 1.3 l/s to 6.6 l/s (20 to 100 USGPM). Ball type valves were used throughout for control of the ambient recharge, jet discharge, and water levels in the square containment tank.

Flow visualization was accomplished with fluorescene dye injected into the jet discharge line by a small peristaltic dosing pump with a flow range of 0. 01 to 1 l/s. Flow illumination was provided by a 4 Watt argon ion laser, with the laser sheet produced by an resonant scanning mirror controlled by a function generator. Image recording was done with both a 35 mm still camera, and video camera, under dark room conditions. Prior to the commencement of an experiment a scale was placed in the same plane that the laser sheet would be illuminating, and photographed to allow later measurement from the

recorded images. Once the scale had been photographed, the position and focal length of the cameras were not changed.

3. 2. 2.   Experimental Procedure

For each H/D ratio, a series of three different densimetric Froude numbers, F_o, were run to investigate the behaviour of the flow. These different F_o were accomplished primarily by varying the jet discharge, since there was no practical means to control the temperatures of either the ambient or the jet. Temperatures of both the ambient and jet were measured before and after experiments, and were used to determine the appropriate discharge for the F_o of that experiment.

Details of the experiments conducted are provided in Table 3.1. The experimental parameters of the diameter (D), total depth to nozzle diameter ratio (H/D), depth over nozzle to nozzle diameter ratio (h_1/D) and densimetric Froude number (F_o) are provided. The recorded temperatures of the ambient water (T_A) and the jet (T_J) were essentially constant at 9°C and 49°C, respectively. The following calculated quantities of the jet are also included; jet flow rate (Q), predicted entrained flow rate (Q_e), modified gravitational constant (g'_o), Froude number (F), and Reynolds' number (R_e). The ambient recharge rate (Q_R) used is also included in Table 3.1.

The entrained flow (Q_e), was estimated by using the method described in Section 3.1. The jet discharge was subtracted from the total flow occurring at the radius coinciding with the wall of the circular tank, to obtain the flow entrained by the jet. The ambient recharge (Q_R) was then set to this flow. As this ambient flow was only an estimate, with the possibility of considerable error due to the crude nature of the model, the sensitivity of the flow behaviour to the rate of ambient recharge was investigated by using ambient recharge flows both greater than and less than that estimated.

At the larger nozzle diameters, the estimated ambient entrainment rate for some jet discharges was well above the capacity of the cold water supply. Experiments for which a

sufficiently high flow rate to match predicted entrainment could not be provided are so indicated in Table 3.1. For these cases, a range of ambient recharge rates from 4 to 6 l/s were utilized.

For all experiments, the jet was started some time before dye injection began, usually 2-3 min. This allowed the flow structure to achieve a near steady state before flow visualization began. Increasing dye concentration in the ambient would have precluded observation of the steady state flow structure if dye injection had commenced simultaneously with the jet flow.

The scientific laser was set up to provide a sheet of laser light along the tank centerline. With both the ambient recharge flow and jet flow adjusted to the desired rates, dye injection would commence. Using the variable speed dosing pump, the concentration of dye in the jet could be adjusted to allow the best visualization of the details of the flow structures, see Figures 4.14 etc. Both video and still images of the flow were recorded for later analysis.

Further experiments were conducted with the ambient recharge flow completely cutoff, and the water level in the tank set slightly below that of the circular walls. These experiments were intended to investigate the occurrence of a radial internal hydraulic jump under choked conditions. The experimental procedure in these cases was essentially the same as that discussed above, with the exception of the ambient recharge being shut off. Also, experiments were conducted for each F_o, in which 15 cm extensions were attached to the nozzles, with the result that h_1 was approximately 15 cm while H remained at 30 cm. This allowed the investigation of the effect of reduced entrainment length in the vertical jet on the radial flow behaviour. These experiments were run with three densimetric Froude numbers for each jet diameter.

Chapter 4

Results and Comments

4. 1. Results

4. 1. 1. Standard Experiments

No radial internal hydraulic jumps were observed in any experiments. Typically, there existed a region immediately outside the surface impingement zone in which instabilities or vortices caused violent, high energy mixing and entrainment, which penetrated the entire depth of the upper layer. At some distance from the discharge point, this violent mixing would collapse, and only smaller, less vigorous, interfacial instabilities were observed. This area was assumed to represent the transition from near-field to far-field conditions. These instabilities would become less pronounced with increasing radius.

Figures 4.14 A-D, from experiment 15020-2 (F_o = 20, H/D = 15) present photographs of the surface flow. Large scale interfacial instabilities, vortex cells, visible as the brightest areas, are apparent starting from the exit from the surface impingement zone at the left. Ambient (darker) fluid can be seen intruding almost to the free surface between the vortex cells. As the cells move outward (to the right), they grow in size, until, just beyond the extreme right of the photographs, the vortex structure breaks down. The translation of vortex cells can be seen in the movement of features **a** and **b** in the sequential photographs. Feature **c** is a wisp of upper layer fluid caught between the surface flow and the underlying inward flow, and as a result, it does not move significantly over the sequence of photos.

The dynamic nature of the flow, the motion of the vortices, and entrainment of ambient fluid, is most apparent when the flow can be seen moving, either viewed first hand or on video recording. The point of transition, not visible on the still photographs, as it was just outside the field of view of the still camere, is easily discernable when the video

recordings are viewed. The rotating, or swirling, motion of the vortices can be clearly seen to collapse into a more uniform and continuous upper layer. Though referred to as a point of transition, the transition from near-field to far-field conditions more correctly occurs over some distance, varying from approximately 5 to 10 cm, depending on the magnitude of the flow.

At any given instant, a distinct, uniform surface layer did not exist in the near-field. The thickness of the upper layer varied constantly as vortices would form, grow while moving outward, and collapse. In addition, examination of the video recordings revealed that the vortices or billows tended to slow as the transition from near-field to far-field conditions was approached.

Observations of the video recordings revealed that the ring vortices in the radially spreading flow originated from the vortices or billows formed in the interfacial regions of the vertical buoyant jet. Billows in the vertical jet could be clearly seen to travel upward into the surface impingment region, to then emerge in the radial flow. The billows were continuous in nature from the vertical to the radial flow. Again, this phenomena is not apparent in the still photographs, and is only apparent when the actual motion can be observed.

With the larger nozzle diameters and small jet momentum in experiments 5002, and 5004, a noticeable oscillation of the vertical jet occurred. The vertical jet tended to oscillate back and forth in a sinusoidal shape about the jet centerline, referred to as a varicose mode. This was likely due to the presence of an asymmetrical helical instability around the jet, this asymmetrical structure would produce unbalanced forces which would account for this behaviour.

As discussed in Chapter 3, a range of ambient recharge flows from the ring diffuser were used to allow for the possibility of error in the predicted entrainment flow rates. The flow structure in the upper layer did not change appreciably with the variation in ambient flow rate. The only significant effect of the lower ambient flow rates was that the dye

concentration in the ambient increased more quickly than with the other experiments, with the result that these experiments were of shorter duration than when the ambient flows were high enough to meet predicted entrainment. At the walls of the circular tank a portion of the flow was drawn down and back toward the vertical jet by the need to compensate for the deficit in ambient flow for entrainment. This resulted in the increase in dye concentration in the ambient fluid observed in these experiments. Since the portion deflected back by the circular wall was still slightly buoyant with respect to the ambient fluid, it tended to exist as a partial third layer between the radially spreading surface buoyant jet and the ambient. As this intermediate flow approached the center of the tank it tended to disappear due to entrainment into the upper layer, and mixing into the ambient fluid.

At no time during these experiments was a radial internal hydraulic jump observed. The behaviour of the upper layer was observed to be as with the other experiments where re-entrainment was not occurring, the only difference being that the surface flow became difficult to distinguish more quickly due to the build up of dye in the intermediate layer and ambient. A minor degree of recirculation at the walls, resulting in a slow dye build up, was observed with all other experiments. While the majority of entrainment was into the upper layer, a small quantity of the upper layer flow was entrained into the lower layer. This minor entrainment into the lower layer resulted in a gradual build up of dye in the lower layer.

As was discussed in Chapter 3, the circular weir did not act as an internal control. The weir's only effect was as a free surface control on the upper layer, which spilled over it. Since the weir could not influence the lower layer, which flowed away from it, the weir could not have acted as an internal control. The minor degree of recirculation observed at the weir was due largely to the exchange of fluid between the two layers, which resulted in a small quantity of upper layer fluid being entrained and mixed into the lower layer. The

entrainment and mixing occurring was heavily biased into the upper layer, but a small proportion of upper layer fluid did end up in the lower layer of fluid.

When large scale re-circulation did occur at the wall, it was due to the inadequacy of the ambient fluid recharge flows from the ring diffuser. The entrainment demands of the radially spreading upper layer were satisified by drawing upper layer fluid down into the lower layer at the circular weir, to eventually be re-entrained back into the upper layer flow. This effect was not one of an internal control imposed by the circular weir, but one that arose because there was not an infinite ambient from which large entrainment flows could be drawn.

4. 1. 2.   Experiments with Nozzle Extensions

The shorter entrainment length in the vertical jet, resulting from the use of the nozzle extensions, produced differences in the structure of the radially spreading surface flow. With less ambient fluid entrained prior to exiting the surface impingement region, the momentum remained concentrated in a smaller volume of fluid than had been the case where the nozzle extensions were not utilized. When nozzle extensions were used the radially spreading surface flow was thinner, and the billows had higher velocities, than was the case for comparable experiments. The point of transition from near-field to far-field conditions tended to be moved outward when nozzle extensions were used.

A modified form of behaviour was noted in the experiments for which the nozzle extension was utilized, and the jet momentum was relatively high. In these cases, the momentum of the fluid moving outward and downward from the surface impingement zone was great enough to cause a "plunge ring", where the buoyant fluid penetrated fairly far down into the lower layer before buoyancy caused it to return upwards, and enter into a normal near-field layer as described above. A photograph of this phenomena is provided in Figure 4.15. This phenomena was observed in experiments 7510-4, 7520-4 and 15020-4, where high jet momentum was combined with the smaller h_1 produced by the nozzle

extensions. The Froude numbers (F), and H/D ratios for these experiments are plotted against the stability criteria of Labridis (1989) in Figure 4.15. From Figure 4.15 it appears that these experiments were ones in which instability and the occurrence of a recirculating near-field was approached. Application of Labridis's stability criteria to these three experiments is approximate, since this criteria does not account for the presence of the nozzle extensions ($H \neq h_1$) used in the experiments in question, which would explain why experiment 7520-4 plots in the unstable region when in fact it was a stable flow. All other series of experiments were within the stable region, and are plotted on Figure 4.15 for comparison purposes.

The high jet momentum and small h_1 of experiments 7520-4, and 7510-4, also produced an extremely large surface disturbance, with resulting large surface waves spreading outward from the center, and then being reflected back by the circular walls. These surface waves are apparent in Figure 4.16. The flow structure in the surface spreading layer was somewhat disrupted by these waves, tending to break up into a series of large billows which only moved slowly outward from the center. The thickness of the upper layer also remained relatively constant in these cases.

4.1.3. Choked Experiments

Chen (1980) reported that a radial internal hydraulic jump would form after some time when the surface flow was completely blocked. Experiments conducted in this study, in which the ambient recharge flow was shut off, and starting water level was below the circular tank wall, failed to produce any internal hydraulic jumps. These experiments were not of as long a duration as Chen's, since there was only a limited volume before the tank would fill and overflow the sides, and the blocking effect would be removed. There was a gradual build up of dye in the experimental tank, but even after some time, internal hydraulic jumps were not observed to have formed for any of the choked experiments. Experiments 15020-C, 7520-C, and 5008-C, were choked experiments.

`Figure 4.17 A-D presents photographs of the flow under choked conditions for the same F_0 and H/D as that for Figure 4.14 A-D. The overall structure of the upper layer flow remains the same as for the experiment featured in Figure 4.14 A-D, however, the intrusion of the intermediate layer described above is apparent in the lower right region of the photographs.

4. 1. 4.   Measured Quantities

Though the main emphasis of this study was on investigation of the flow structure by flow visualization techniques, it was possible to obtain some preliminary data from the recorded images. Using the still photographs and video recordings it was possible to measure certain quantities of the radially spreading surface flow. These quantities are; average billow spacing (S), depth of flow at exit from surface impingement zone (h_{um}), approximate speed of movement of billows (U_b), radius at which transition from near-field to far-field occurs (R_t), and average growth rate of the surface layer in the near-field (dh/dr). The frequency at which billows exited the surface impingement zone (B_f), was also determined from the video recordings. The Strouhal Number $(S_r = B_f D/U)$ of the radial flow, which expresses the billow frequency relative to the jet parameters U and D, was calculated for each experiment. Data obtained for each of these quantities are provided in Table 4.2. Figure 2.6 was used to predict the thickness of the upper layer (h_{up}) at the exit from the surface impingement zone, for comparison to measured values.

With experiments in the 5002, 5004, and 5008 series, encompassing the largest jet diameter and highest jet flow rates, consistent results were not apparent in the measured quantities for the radially spreading surface region. The flow structure does not appear to be different in form from the other experiments, it is possible that shallow water effects are causing a change in the trends in upper layer growth rate and upper layer depth from that observed in the other experiments. However, the preliminary nature of this study prevents any further analysis of this phenomena, as sufficient data is not available to allow a more

complete consideration of these experiments. As a result, data regarding upper layer depth (h_{um}), and upper layer growth rate (dh/dr), are considered unreliable, and are not discussed further.

At the larger jet diameters and higher jet flow rates, covering experiments in series 7510, 7520, and 5008, the radius at which the apparent transition from near-field to far-field conditions occurs is nearly constant at 65-70 cm. It appears then, that the tank walls are forcing a change in the flow conditions at smaller radii than would occur in an infinite ambient for these jet parameters.

In Figure 4.18, the Strouhal number of the radial flow was plotted against the densimetric Froude number. As can be seen by examining Figure 4.18, the frequency of the billows in the radial flow decreases relative to the jet parameter U and D (D being fixed for each H/D ratio) with increasing densimetric Froude number, for all depth to nozzle diameter ratios. As the densimetric Froude number is increased significantly above 10, the Strouhal numbers for all H/D ratios appear to converge. Nozzle extensions result in higher Strouhal numbers than for the corresponding experiments without nozzle extensions. A possible cause for the decrease in S_r with increasing F_o, is that the higher flow rates are accomodated by larger billows. While Table 4.2 indicates that the actual frequency of billows, B_f, does increase with F_o, it does not increase as quickly as U, resulting in a decease in S_r. At lower Froude numbers, an increase in the H/D ratio results in a lower S_r. In this case, this can be assumed to translate directly into a decrease in the billow frequency. This may occur, since a greater depth allows pairing of instabilities to occur in the vertical jet, with the result that there are fewer instabilities which are farther apart. This is then reflected in the frequency of billows exiting the surface impingement region. The convergence of the various curves as F_o is increased indicates that the depth ratio is of decreasing importance as F_o increases above 10. The slope of the curves also decreases with increasing F_o, indicating that S_r may be constant for very large F_o.

The upper layer depth at the exit from the surface impingement zone was plotted against F_o (Figure 4.19), after non-dimensionalizing with respect to D ($h_u = h_u/D$). Both measured values, and predicted values, from Figure 2.6 (Lee & Jirka, 1981), are included. When F_o is increasing, h_u increases. The increase in the upper layer depth with increased F_o, is due to the increased volume flux, the depth of the radial flow and the size of the associated instabilities are increased to accomodate the increased flow. Decreasing H/D results in a decrease in h_u with fixed F_o. The decrease in entrainment length reduces the entrained volume in the vertical jet, with the result that the upper layer thickness at the exit from the surface impingment zone is reduced. There is little correlation between the predicted curves and the measured curves.

Figure 4.20 is a plot of the upper layer depth data, from each series of experiments in this study, on to the predicted solutions by Lee & Jirka (1981) for upper layer depth at the exit from the surface impingement zone. For this plot the upper layer depth has been non-dimensionalized by dividing by the total water depth, H. In comparing the observed values to the solutions of Lee & Jirka (1981), it is apparent that there is little correlation.

Figure 4.21 presents a plot of the average rate of upper layer growth against the densimetric Froude number. For the two series of experiments with the larger depth ratios, $H/D = 15$ and $H/D = 7.5$, the rate of upper layer growth decreases with increasing F_o. One might expect that the upper layer growth rate should increase with increasing F_o. However, there is a possible explanation for the decrease in upper layer growth rate with increasing F_o. As the volumetric flow rate is increased (as a result of increasing F_o), the velocities in both the upper and lower layer are increased. The lower layer velocity increases to meet the increased entrainment demands of both the vertical jet region, and the radially spreading regions. In the upper layer, the velocity increase is much greater than the lower layer, since the flow in the upper layer is composed of both the jet flow and the entrainment flow, both of which are increased by an increase in F_o. There is a slight increase in upper layer thickness with F_o, but not enough to negate the higher velocities

due to the higher volumetric flow rates. Since the increase in velocity in the upper layer is greater than the increase in velocity in the lower layer, there is a net increase in the convection speed of the instabilities. Thus, while the instabilites or vortices are increasing in size at a faster rate (dh/dt increases), the change in size with distance (dh/dr) is reduced by the increase in convection speed. The billows are being swept along. This effect is apparent when one considers the variation in billow speed (U_b) with increasing F_o in Table 4.2.

The use of nozzle extensions is reflected in a decrease in the upper layer growth rate from that for the experiments where the nozzle extensions were not utilized. With the nozzle extensions, the entrainment in the vertical jet is reduced, and hence the flow in the radial region is less than it would be without the nozzle extensions. The lesser flow in the upper layer reduces interfacial shear, and therefore entrainment, resulting in a lower upper layer growth rate. The effect of a smaller H/D ratio for a given F_o is similar, entrainment in the vertical region is reduced, which reduces the upper layer growth rate.

4. 2. Comment on Results

A large range of flow conditions has been examined and under none of these conditions were radial internal hydraulic jumps observed. This result is in agreement with that of Wood & Wilkinson (1971) for a long channel, where it was found that an internal hydraulic jump would only form when a downstream sill or hump was placed in the channel. In the absence of a strong internal control only an entrainment zone will be present. The results of Chen (1980), and Lawrence (1985), and the predictions of Lawrence & Bratkovitch (1993), also support this result.

In all experiments, except 7510-4, 7520-4 and 15020-4, a radial form of entraining shear layer was observed. In the near-field region, violent mixing and entrainment occurred in the form of instabilities or vortices which penetrated the full depth of the upper layer. These vortices were continuations of the instabilities formed in the

vertical buoyant jet region. At the transition to far-field conditions this violent mixing was observed to collapse, to be replaced by a stable upper layer with smaller instabilities at the interface between the upper layer and lower ambient layer. Even when the experiment was contained within the circular walls, and no replenishment flow was provided, the above described flow structure was still observed. However, dye concentrations increased very quickly, precluding the observation of flow structure as unstable conditions were approached due to warming of the ambient.

When ambient recharge flows were too low to meet demand, the deficit was made up for by recirculation of upper layer fluid at the walls. This resulted in the gradual increase in dye concentration in the ambient. Even when this recirculation occurred no radial internal hydraulic jumps were observed. The existence of the recirculation and intermediate layer was entirely due to the presence of the circular wall forcing flow back to meet entrainment demands, since ambient flow was not sufficient, and hence was entirely artificial. If the circular wall had not been present, as in a genuine infinite ambient, this structure would not have been observed.

Because the densities of the ambient and jet fluid could not be controlled, the effects of varying the buoyancy and momentum/volume fluxes independently of each other could not be investigated. Therefore, the results obtained with varying F_o more realistically represent the effects of varying volumetric flow rates with fixed density differences, and not the behaviour of the flow under varying momentum and buoyancy conditions.

It should be noted that there was not a distinct interface in the two layer flow in the near-field. Instead the upper layer flow took the form of a series of instabilities which propogated outward from the surface impingement region. Only once the far-field was reached, did the flow settle down and a distinct stable interface form. The nature of the flow in the near-field means that conventional internal hydraulic principles do not apply to the flow. A continuous upper layer does not exist, which implies that internal long waves

are not a possibility, since there is not an interface for them to act along. Since internal long waves cannot exist in the near-field, and cannot govern the flow, and the concepts of internally supercritical and internally subcritical flow are hard to apply, this effectively precludes the existence of internal hydraulic jumps. While it would be possible to determine a composite Froude number (G), based on the time averaged velocities, depths, and effective gravitational accelerations of the flow, this quantity would have little relevance. The application of standard hydraulic equations, such as continuity and momentum, while possible on a time-averaged basis, do little to indicate the flow conditions in the upper layer due to its discontinuous, intermittent, nature. For this reason, and since internal hydraulic theory as discussed above is not really applicable, the upper layer flow could be considered to be not truly hydraulic in the traditional sense. The predictions of the composite Froude number carried out in Chapter 3 are irrelevant in light of the above discussion.

4. 3. Comparison to Existing Approaches

The assumption of the presence of a radial internal hydraulic jump by Lee & Jirka (1981) is clearly not appropriate in representing the actual mechanisms and structure present in the radially spreading flow. Lee & Jirka (1981) conducted experiments to aid in adjusting their model. They relied on an arrangement where the flow out of the experimental tank was partially or completely choked by matting at the outflow weir. Thus, their model is probably inaccurate, due to having been based on the assumption of an internal hydraulic jump, and also having been calibrated using a choked flow in which atypical conditions existed. Choked conditions similar to those of Lee & Jirka (1981) were not possible to reproduce in this study due to the configuration of the apparatus and the inability to produce steady state conditions in the choked experiments of this study. Steady state conditions could not be established in the choked experiments undertaken in this study as the choked conditions were produced by starting the experiment with the

ambient water level below the level of the circular weir. After a short period of time had passed, the tank would fill, and flow over the weir would occur, eliminating the choked conditions.

Wright et al. (1991) was more accurate in recognizing the possibility of entrainment into the radially spreading surface flow, but their model was still based on the existence of an internal hydraulic jump in a portion of the near-field. Wright's other main assumption, that the flow becomes internally critical in the far-field, could not be verified at this point, since velocity measurements are not available from this study, or from Wright et al. (1991). Wright's observations of ring vortices, which propagated outward from the surface impingement region before collapse, were confirmed.

Both Lee & Jirka (1981), and Wright et al. (1991) may assume the presence of an internal hydraulic jump because of the manner in which they conducted their experiments. In neither of these investigations was a thin cross-section of the flow examined using flow-visualization techniques similar to those used in this study, these techniques having only recently become practical to implement with the availability of lasers and advanced video recording equipment. Both were viewing the flow in bulk, and were not able to distinguish the fine details of the flow structure. From the side, or above, the radial buoyant jet region would appear to be a near-continuous layer which increased in thickness with distance until the far-field was reached, and as such could be mistaken for an internal hydraulic jump.

Lawrence & Bratkovitch (1993) correctly identified the existence of the entrainment zone comprising the near field, and the existence of entrainment to a lesser degree in the far-field. Although the assumption of the entrainment zone was correct, the accuracy of the model, as for the other models discussed above, in predicting the dilution and flows was not investigated, and no comment can be made on its effectiveness. Lawrence & Bratkovitch (1993) assume the existence of a distinct upper layer in the near-

field, as do the other models. This may be a useful approximation of the time-averaged behaviour of the flow, but it does not explicitly recognize the actual mechanisms present.

In comparing the thickness of the radial surface jet at the exit from the surface impingement zone (h_{um}) to the predicted thickness of the surface impingement zone (h_{up}), (refer to Figure 4.19 and Figure 4.20) it appears that there is little correlation between the solutions of Lee & Jirka (1981) and the measured values.

A graphical comparison of the range of experiments undertaken in this study with those undertaken by Lee & Jirka (1981), and Wright et al. (1991), is provided in Figure 4.22. Wright et al. (1991) used a range of Froude numbers from 1.5 to greater than 1000, in combination with small nozzle diameters (2.2 and 4.7 mm), and large flow rates and density deficits. Most of Wright et al.'s experiments utilized depth ratios greater than 80, with none less than 15. Lee & Jirka's (1981) experiments had a similar range of parameters, but did use depth ratios as low as 2. The experiments of this study utilized a range of densimetric Froude numbers from 2 to 20, and depth ratios from 5 to 15, and occupy an envelope essentially missed by the two other studies mentioned here. In many cases, Wright et al.'s experiments utilized parameters (F_o and H/D) well in excess of those in this study, however the mechanisms investigated in this study are alluded to by Wright et al.'s reference to ring vortices, indicating that the results of this study are applicable beyond the range of this study.

Since this study did not collect numerical data regarding the dilution or velocity profiles in the radially spreading surface flow, it is not possible to comment on the accuracy of the models discussed above in modeling the flow. The results of this study are of a preliminary nature and are focussed mainly on identifying the details of the flow structure in the radially spreading surface layer. Future investigations will be of greater scope and will include evaluation and refinement of the numerical output of the models discussed above.

4. 4. Restrictions and Other Problems

In spite of the apparatus being designed in an effort to achieve a steady state experiment that could be operated indefinitely, any given run was limited to 5 minutes or less before dye build up in the ambient would make flow visualization impossible. At the walls of the circular tank, it was observed that some of the surface layer would be carried downward and back into the ambient, instead of over the sides to waste. This recirculation effect would occur to compensate for any deficit between the volume being entrained and the ambient recharge flow being provided. A minor degree of recirculation occurred in all experiments, whether a deficit in available ambient fluid occurred or not, due to the entrainment of upper layer fluid into the lower ambient layer. This fluid would be diverted down and back into the tank at the wall, to become mixed with the ambient fluid. This resulted in a gradual dye build up, limiting the life of experiments. This effect might be eliminated by attaching matting or filter material to the inside of the circular wall, just below the crest, to stifle downward currents at the wall.

The range of experimental flows that could be utilized was smaller than expected. This was due to the cold water supply not being capable of providing enough flow to meet the entrainment demands of the jet discharge at its higher flow rates, and hence recirculation effects set in during these experiments, necessitating the use of lower densimetric Froude numbers with the larger jet orifices, in order to avoid it. Also there tended to be large scale surface disturbances when high jet flow rates and large jet diameters were utilized.

The range of conditions which could be investigated was also limited by the temperatures of the cold and hot water supplies. Since these temperatures were essentially beyond the control of the researcher, and remained constant during the period in which experiments were being conducted, it was not possible to change the ratio of F to F_o. This had the result that the buoyancy of the jet could not be varied independently

of momentum. As a result, the behaviour of extremely buoyant jets or of unstable or nearly unstable flows could not be investigated. Modification of the experimental apparatus to allow salt injection in the jet, or control of the jet temperature, would overcome this limitation.

Chapter 5

Conclusions and Recommendations

When a vertical buoyant jet enters shallow water there are four distinct regions: the vertical buoyant jet region, the surface impingement region, the momentum dominated near-field and the buoyancy dominated far-field. As the flow exits the surface impingement region there will be entrainment of ambient fluid, and an increase in the thickness of the radial surface flow as it spreads outward. An internal hydraulic jump does not occur as part of this flow. The radially spreading surface layer exists as a series of ring vortices or instabilities which propagate outward, until the far-field is reached, and they collapse into a continuous, more stable layer. The far-field is characterized by a sharper and more stable interface between the two layers, with smaller, less vigorous instabilities, which are remnants of the more active interface in the near-field region. The upper layer flow in the near-field is an intermittent dynamic flow, lacking a continuous distinct interface, which makes the occurrence of internal hydraulic jumps impossible.

The present study represents a preliminary investigation to identify, and explain, the mechanisms of the radially spreading surface flow associated with the discharge of a buoyant jet in shallow water. As such, collection of detailed data regarding velocity distributions and dilutions in the radially spreading surface layer was not undertaken. Nevertheless, the results of the present study serve to improve the understanding of the mechanisms, and behaviour, of radially spreading surface flows resulting from the discharge of a vertical jet in shallow water. Experimental investigation of these flows in the past had been limited. With the increased knowledge of the structure of radial flows arising out of this investigation, existing models used for predictive purposes can be improved or refined. This in turn should result in more efficient design of outfalls, and better protection of receiving water environments.

The transition to far-field conditions from the near-field is accomplished by gradual entrainment and mixing into the upper layer, as described above. Even during extreme flow conditions, in which the upper layer is completely blocked off, a radial internal hydraulic jump did not occur. While preliminary in nature, the results of this study raise questions as to the accuracy of some models, such as Lee & Jirka (1981), Wright et al. (1991), and their derivatives, which were formulated based on the assumption of the occurrence of a radial internal hydraulic jump in the transition from momentum dominated to buoyancy dominated conditions. The general predictions by Lawrence & Bratkovitch (1993) as to the nature of the flow have been confirmed.

Due to decreased entrainment length in the vertical jet region at lower depth to nozzle diameter ratios, the surface layer would be thinner, and velocities of the billows/vortices would be higher, than would occur at larger depth to nozzle diameter ratios. The depth of the surface layer at the exit from the surface impingement region and velocity of the billows was shown to increase with increasing densimetric Froude number. Flow structures were not significantly affected by variation in the ambient recharge rates in the experimental tank.

High densimetric Froude numbers (>10), in combination with short entrainment lengths in the vertical jet due to the use of nozzle extensions, were found to produce a different structure in the radially spreading surface layer. The surface boil was more pronounced, and there was a ring of buoyant fluid immediately outside the surface impingement zone, which protruded downwards into the ambient fluid as far as half the water depth. The flow exited this "plunge ring" into a radially spreading surface layer characterized by billows larger than occurred in the unmodified experiments, and a thicker surface layer which had nearly constant depth. These flow conditions represent the approach to a recirculating flow regime.

As the jet densimetric Froude number is increased, the Strouhal number decreases. This indicates that the billow frequency of the upper layer decreases with respect to the jet

velocity as the Froude number increases. The Strouhal number will increase, if, for a given densimetric Froude number, the ratio of the water depth to the jet nozzle diameter is decreased. This effect arises because in the shorter entrainment length in the vertical jet, less pairing or merging of billows occurs. The billows in the radial flow at the exit from the surface impingement zone are directly linked to those in the vertical jet. The effect of the depth ratio was found to decrease sharply as the densimetric Froude number was increased above approximately 10.

Lee & Jirka (1981) provided a graph (Figure 2.6) for estimating the thickness of the surface blocking layer as a function of the densimetric Froude number (F_o), and the depth to nozzle diameter ratio (H/D). When compared to the experimentally measured thickness of the surface layer at the exit from the surface impingement region, the graph was found to be inaccurate for most flows, particularly those with small H/D (5 or 7.5) where the error was as much as 50%.

As the densimetric Froude number is increased for a given depth ratio, the growth rate of the upper layer is decreased, due to an increase in the convection speed of the instabilities. A change in the depth ratio for a given densimetric Froude number results in an opposite change in the upper layer growth rate. The change in the entrainment length in the vertical jet region accounts for this effect.

Further experimental work involving measurement of dilution and velocities in the radially spreading layer can be undertaken. Direct comparison to the predictions provided by existing models would then make possible evaluation and refinement of these models in detail. The experimental apparatus should be modified to enable changing the buoyancy of the jet, allowing the effects of variations in buoyancy and momentum to be fully studied over a wider range of flow conditions. Dilution and surface layer behaviour in a recirculating regime, or with a very stable jet, may then be investigated. The effect of buoyancy and momentum variation on the frequency of billow generation, and the growth

rate of the upper layer, should be investigated. Further refinement of the circular tank to eliminate or minimize the recirculation effect at the tank wall should be considered.

Notation

α : entrainment coefficient

α : growth rate coefficient (in Equation 2. 31)

α_j : jet entrainment coefficient

α_p : plume entrainment coefficient

$B = Ug' \, \pi D^2 / 4$: initial buoyancy flux of jet (Equation 2. 6)

$b_t = 0.127z$: characteristic width of tracer profile (Equation 2. 11)

$b_u = 0.107z$: characteristic width of velocity profile (Equation 2. 10)

B_f : billow frequency at exit from surface impingement zone

$\beta = \int_A g' u \, \mathrm{d}A$: specific buoyancy flux in jet (Equation 2. 3)

C : tracer concentration

C_o : initial tracer concentration

$C_m = 5.64 C_o \left(l_Q / z \right)$: tracer concentration on jet centerline (Equation 2. 13)

$c_p = 0.254$: plume coefficient

D : diameter of jet nozzle

d_s : depth of upper layer at exit from surface impingement region (measured)

$\Delta \rho$: density difference between ambient and jet

$\dfrac{\overline{dh}}{dr}$: average growth rate of radially spreading upper layer (measured)

$\dfrac{dh}{dr} = \alpha v_r \left(1 - \dfrac{Ri}{Ri_c} \right)$: upper layer growth rate (Equation 2. 31)

$F_o = U / \left(g'_o D \right)^{1/2}$: jet densimetric Froude number

$F = U / \left(gD \right)^{1/2}$: jet Froude number

$G^2 = \dfrac{\overline{U}^2}{g' h_u} + \dfrac{\overline{U}^2_{rel}}{g' \left(H - h_u \right)}$: composite Froude number squared (Equation 2. 32)

$g'_o = g \, \Delta \rho_o / \rho$: initial effective gravitational acceleration

$g' = g \, \Delta \rho / \rho$: effective gravitational acceleration

$g'_i = g'_o \, Q/Q_i$: effective gravitational acceleration at section i (Equation 3. 37)

g'_1: effective gravitational acceleration at entrance to surface impingement region

H: total depth of ambient water

h_s : height of surface hump

h_u: depth of upper layer

$\mathbf{h_*} = h_u/D$: non-dimensionalized upper layer depth, at exit from surface impingment zone

h_1: depth of water above jet nozzle

$l_Q = Q/M^{1/2}$: jet characteristic length scale (Equation 2. 8)

$l_M = M^{3/4}/B^{1/2}$: characteristic length scale for buoyant jets (Equation 2. 17)

$M = U^2 \, \pi D^2/4$:initial momentum flux of jet (Equation 2. 5)

M_1: momentum flux at entrance to surface impingement region

$m = \int_A u^2 dA$: specific momentum flux in jet (Equation 2. 2)

$Q = U \, \pi D^2/4$: initial volume flux of jet (Equation 2. 4)

Q_e : estimated entrained flow

Q_R : ambient recharge flow rate

Q_1 : volume flux at entrance to surface impingement region

$Q_{e_i} = Q_i - Q$: entrained flow at section i (Equation 3. 34)

Q_i : total flow at section i

$\mu = \int_A u dA$: specific volume flux in jet (Equation 2. 1)

$\mu = 0.254 m^{1/2} z$: specific volume flux in plume (Equation 2. 16)

Re: jet Reynolds' number at exit from nozzle

$R_i = \dfrac{g' h_u}{\Delta U^2}$: bulk Richardson number

$R_o = l_Q/l_M$: initial jet Richardson number (Equation 2. 18)

R_p : plume Richardson number

R_t: radius at which transition from near-field to far-field conditions occurs (measured)

$R_u = \dfrac{Q/(2\pi r_i)}{\nu}$: Reynolds' number of upper layer flow (Equation 3. 40)

r_i: radius at section i

r_1: radius of jet at entrance to surface impingement region

r_2 : radius at exit from surface impingement region

U : average velocity at jet exit

S: average billow spacing (measured)

$S_r = B_f D/U$: Strouhal number of radially spreading flow

T_j : temperature of jet fluid at nozzle exit

T_A : temperature of ambient fluid

U_b : average velocity of billows (measured)

$\overline{U}$: averaged velocity in upper layer of radially spreading flow

$\overline{U}_{ret}$:averaged return velocity in layer below radially spreading flow

u : time averaged jet velocity

$u_c = 7.0\, l_Q M/zQ$: time averaged velocity at jet center line (Equation 2. 9)

u_1 : velocity in jet at entrance to surface impingement region, assuming top hat velocity profile (Lawrence & Bratkovitch, 1993)

$$v_r = \frac{\overline{U} - \overline{U}_{ret}}{\left(\overline{U} + \overline{U}_{ret}\right)}: \text{velocity ratio for two layer flow}$$

v: kinematic viscosity

z : distance along jet centerline

z_t : length of Zone of Flow Establishment

$Z_t = z_t/D$: non-dimensionalized length of Zone of Flow Establishment

z_e: entrainment length

$Z_e = z_t/D$: non-dimensionalized entrainment length

References

Abraham, G. 1965. "Entrainment Principle and its Restriction to Solve Jet Problems", *Journal of Hydraulic Research*, Vol. **3**, No. 2, pp. 1-23.

Alavian,, V. , Hoopes, J. A. 1982. "Thermal Fronts in Heated Water Discharges", *Journal of the Hydraulics Division, ASCE*, Vol. **108**, pp. 707-725.

Andreopoulos, J. , Praturi, A. , Rodi, W. 1986. "Experiments on Vertical Plane Buoyant Jets in Shallow Water", *Journal of Fluid Mechanics*, Vol. **168**, pp 305-336.

Chen, J. C. 1980. *"Studies on Gravitational Spreading Currents"*, W. H. Keck Laboratory Report No. KH-R-40, California Institute of Technology, Pasadena, California, 436 pp. .

Crow, S. C. , Champagne, F. H. 1971. , "Orderly Structure in Jet Turbulence", *Journal of Fluid Mechanics*, Vol. **48**, pp 547-591.

Daugherty, R. L. , Franzini, J. B. , Finnemore, E. J. 1985. *"Fluid Mechanics with Engineering Applications"*, 8th edition, McGraw-Hill, New York, 583 pp. .

Fischer, H. B. , List, E. J. , Imberger, J. , Koh, R. C. Y, Brooks, N. H. 1979. *"Mixing in Inland and Coastal Waters"*, Academic Press, New York, 483 pp. .

Garvine, R. W. 1984. "Radial Spreading of Buoyant, Surface Plumes in Coastal Waters", *Journal of Geophysics Research*, Vol. **89**, No. C2, pp. 1989-1996.

Jirka, G. H. , Harleman, D. R. F. 1979. "Stability and Mixing of a Vertical Plane Buoyant Jet in Confined Depth", *Journal of Fluid Mechanics*, Vol. **94**, part 2, pp. 275-304.

Koh, R. C. Y. 1971. "Two-dimensional surface warm jets", *Journal of the Hydraulics Division, ASCE*, Vol. **97**, HY6, pp. 819-836.

Koop, C. G. and Browand, F. K. 1979. "Instability and Turbulence in a Stratified Fluid with Shear", *Journal of Fluid Mechanics.* , Vol. **93**, 135-159.

Labridis, C. 1989. "Buoyant Jet in Shallow Water With a Crossflow", Thesis submitted in partial fulfillment of the degree Master of Applied Science, University of British Columbia, Vancouver, Canada, 57 pp.

Lawrence, G. A. 1985. "The Hydraulics and Mixing of Two-Layer Flow Over an Obstacle", Thesis submitted in partial fulfillment of the degree Doctor of Philosophy, University of California, Berkeley, California. 130 pp.

Lawrence, G. A. , Bratkovitch, A. 1993. "Vertical buoyant jet into very shallow water with current", submitted to: *Journal of Hydraulic Engineering, ASCE.*

Lee, J. H. W, Jirka, G. H. 1981. "Vertical round buoyant jet in shallow water", *Journal of The Hydraulics Division, ASCE,* Vol. **107**, pp. 1651-1675.

List, E. J. , Imberger, J. 1981. "Turbulent entrainment in buoyant jets and plumes", *Journal of the Hydraulics Division, ASCE,* Vol. **99**, pp 1651-1675.

List, E. J. 1982. "Turbulent jets and plumes", *Annual Review of Fluid Mechanics,* Vol. **14**, pp. 189-212.

McClimans, T. A. 1978. "Fronts in Fjords", *Geophysics, Astrophysics and Fluid Dynamics,* Vol. **11**, pp. 23-34.

Murota, A. , Muraoka, K. 1967. "Turbulent diffusion of the vertically upward jet", *Proceedings of the 12th I. A. H. R. Congress,* Vol. **4**, pp. 60-70.

Morton, B. R. , Taylor, G. , Turner, J. S. 1956. "Turbulent gravitational convection from maintained and instantaneous sources", *Proceedings of the Royal Society of London,* Vol. **234(A)**, pp. 1-23.

Rottman, J. W. , Simpson, J. E. 1983. "The initial development of gravity currents from fixed volume releases of heavy fluids", Proceedings of the IUTAM Symposium on Atmospheric Dispersion of Heavy Gases and Small Particles", Delft, The Netherlands, August 1983.

Scarpace, F. L. , Green, T. 1973. "Dynamic surface temperature structure of thermal Plumes", *Water Resources Research,* Vol. **9**, pp. 138-153.

Wilkinson, D. L. , Wood, I. R. 1971. "A rapidly varied flow phenomena in a two layer flow", *Journal of Fluid Mechanics,* Vol. **47**, part 2, pp 241-256.

Wright, S. J. , Roberts, P. J. W. , Zhongmin, Y. , Bradley, N. E. 1991. "Surface dilution of round submerged buoyant jets", *Journal of Hydraulic Research,* Vol. **29**, No. 1, pp. 67-89.

Appendix A

Tables

EXP. No.	Run No.	D cm	H/D	h1/D	Q l/s	Qe l/s	Qr l/s	g' cm/s^2	Fo	F	M cm^4/s^2	Re
1	15005-1	2	15	15	0.08	0.20	0.15	10.9	5	0.53	2000	8400
2	15005-2	2	15	15	0.08	0.20	0.20	10.9	5	0.53	2000	8400
3	15005-3	2	15	15	0.08	0.20	0.25	10.9	5	0.53	2000	8400
4	15005-4	2	15	7.5	0.08	0.20	0.20	10.9	5	0.53	2000	8400
5	15010-1	2	15	15	0.15	2.00	1.50	10.9	10	1.05	7100	16800
6	15010-2	2	15	15	0.15	2.00	2.00	10.9	10	1.05	7100	16800
7	15010-3	2	15	15	0.15	2.00	2.50	10.9	10	1.05	7100	16800
8	15010-4	2	15	7.5	0.15	2.00	2.00	10.9	10	1.05	7100	16800
9	15020-1	2	15	15	0.30	6.00	4.00	10.9	20	2.11	28600	33700
10	15020-2	2	15	15	0.30	6.00	5.00	10.9	20	2.11	28600	33700
11	15020-3	2	15	15	0.30	6.00	6.00	10.9	20	2.11	28600	33700
12	15020-4	2	15	7.5	0.30	6.00	6.00	10.9	20	2.11	28600	33700
13	7505-1	4	7.5	7.5	0.43	2.90	2.20	10.9	5	0.53	14700	23800
14	7505-2	4	7.5	7.5	0.43	2.90	2.90	10.9	5	0.53	14700	23800
15	7505-3	4	7.5	7.5	0.43	2.90	3.60	10.9	5	0.53	14700	23800
16	7505-4	4	7.5	3.7	0.43	2.90	2.90	10.9	5	0.53	14700	23800
17	7510-1*	4	7.5	7.5	0.86	8.60	4.00	10.9	10	1.05	58800	47700
18	7510-2*	4	7.5	7.5	0.86	8.60	5.00	10.9	10	1.05	58800	47700
19	7510-3*	4	7.5	7.5	0.86	8.60	6.00	10.9	10	1.05	58800	47700
20	7510-4*	4	7.5	3.7	0.86	8.60	6.00	10.9	10	1.05	58800	47700
21	7520-1*	4	7.5	7.5	1.70	26.20	4.00	10.9	20	2.11	229900	95500
22	7520-2*	4	7.5	7.5	1.70	26.20	5.00	10.9	20	2.11	229900	95500
23	7520-3*	4	7.5	7.5	1.70	26.20	6.00	10.9	20	2.11	229900	95500
24	7520-4*	4	7.5	3.7	1.70	26.20	6.00	10.9	20	2.11	229900	95500
25	5002-1	6	5	5	0.47	2.00	1.50	10.9	2	0.21	7800	17500
26	5002-2	6	5	5	0.47	2.00	2.00	10.9	2	0.21	7800	17500
27	5002-3	6	5	5	0.47	2.00	2.50	10.9	2	0.21	7800	17500
28	5002-4	6	5	2.5	0.47	2.00	2.00	10.9	2	0.21	7800	17500
29	5004-1	6	5	5	0.94	5.10	4.00	10.9	4	0.42	31200	35000
30	5004-2	6	5	5	0.94	5.10	5.00	10.9	4	0.42	31200	35000
31	5004-3	6	5	5	0.94	5.10	6.00	10.9	4	0.42	31200	35000
32	5004-4	6	5	2.5	0.94	5.10	5.00	10.9	4	0.42	31200	35000
33	5008-1*	6	5	5	1.80	15.60	4.00	10.9	8	0.84	114500	70100
34	5008-2*	6	5	5	1.80	15.60	5.00	10.9	8	0.84	114500	70100
35	5008-3*	6	5	5	1.80	15.60	6.00	10.9	8	0.84	114500	70100
36	5008-4*	6	5	2.5	1.80	15.60	6.00	10.9	8	0.84	114500	70100
37	15020-C	2	15	15	0.30	N/A	0.00	10.9	20	2.11	28600	33700
38	7520-C	4	7.5	7.5	1.70	N/A	0.00	10.9	20	2.11	229900	95500
39	5008-C	6	5	5	1.80	N/A	0.00	10.9	8	0.84	114500	70100

Note: * denotes experimental runs where cold water supply was insufficient to meet predicted entrainment.

Table 3.1 Experiments Conducted

EXP. No.	Run No.	D (cm)	H/D	h1/D	Fo	F	Rt (cm)	hup (cm)	hum (cm)	S (cm)	Ub (cm/s)	Bf (hz)	Sr	dh/dr
1	15005-1	2	15	15	5	0.53	35.00	2.40	2.4	3	6.50	0.8	0.063	0.12
2	15005-2	2	15	15	5	0.53	35.00	2.40	2.4	3	6.50	0.80	0.063	0.12
3	15005-3	2	15	15	5	0.53	35.00	2.40	2.4	3.2	6.50	0.73	0.058	0.11
4	15005-4	2	15	7.5	5	0.53	35.00	2.40	1.5	2.5	7.00	1.00	0.079	0.10
5	15010-1	2	15	15	10	1.05	40.00	2.40	2.7	3	7.50	0.93	0.039	0.11
6	15010-2	2	15	15	10	1.05	40.00	2.40	2.7	3	7.50	0.87	0.036	0.10
7	15010-3	2	15	15	10	1.05	40.00	2.40	2.6	3	7.50	0.93	0.039	0.09
8	15010-4	2	15	7.5	10	1.05	43.00	2.40	2	2.5	8.00	1.00	0.042	0.07
9	15020-1	2	15	15	20	2.11	45.00	2.40	3.2	2.5	8.00	1.00	0.021	0.09
10	15020-2	2	15	15	20	2.11	45.00	2.40	3.2	2.5	8.00	0.93	0.02	0.09
11	15020-3	2	15	15	20	2.11	47.00	2.40	3.1	2.5	8.00	1.00	0.021	0.09
12	15020-4	2	15	7.5	20	2.11	55.00	2.40	N/A	N/A	10.00	N/A	N/A	N/A
13	7505-1	4	7.5	7.5	5	0.53	54.00	2.40	2.7	5.4	7.40	0.87	0.101	0.05
14	7505-2	4	7.5	7.5	5	0.53	56.00	2.40	2.7	5.4	7.40	0.93	0.109	0.05
15	7505-3	4	7.5	7.5	5	0.53	56.00	2.40	2.7	5.4	7.40	0.87	0.101	0.05
16	7505-4	4	7.5	3.7	5	0.53	67.00	2.40	2.2	6	8.00	1.13	0.132	0.04
17	7510-1	4	7.5	7.5	10	1.05	64.00	2.40	3	4	10.00	1.00	0.058	0.06
18	7510-2	4	7.5	7.5	10	1.05	65.00	2.40	3	4	10.00	1.00	0.058	0.06
19	7510-3	4	7.5	7.5	10	1.05	65.00	2.40	3	4	10.00	1.00	0.058	0.06
20	7510-4	4	7.5	3.7	10	1.05	70.00	2.40	N/A	N/A	11.00	1.07	0.062	0.00
21	7520-1	4	7.5	7.5	20	2.11	65.00	2.40	3.2	4	13.00	1.20	0.035	0.02
22	7520-2	4	7.5	7.5	20	2.11	70.00	2.40	3.2	4	13.00	1.13	0.034	0.02
23	7520-3	4	7.5	7.5	20	2.11	70.00	2.40	3.2	4	13.00	1.20	0.035	0.02
24	7520-4	4	7.5	3.7	20	2.11	N/A	2.40	N/A	N/A	N/A	N/A	N/A	N/A
25	5002-1	6	5	5	2	0.21	50.00	2.50	3	8	5.50	0.47	0.168	0.04
26	5002-2	6	5	5	2	0.21	50.00	2.50	3	8.5	5.50	0.53	0.193	0.04
27	5002-3	6	5	5	2	0.21	50.00	2.50	3	8.5	5.50	0.47	0.168	0.04
28	5002-4	6	5	2.5	2	0.21	50.00	2.50	2	7	6.00	0.80	0.289	0.04
29	5004-1	6	5	5	4	0.42	60.00	2.50	4	5	6.50	0.73	0.132	0.05
30	5004-2	6	5	5	4	0.42	60.00	2.50	4	5	6.50	0.73	0.132	0.05
31	5004-3	6	5	5	4	0.42	60.00	2.50	4	5	6.50	0.73	0.132	0.04
32	5004-4	6	5	2.5	4	0.42	65.00	2.50	2.5	4	7.00	1.00	0.18	0.04
33	5008-1	6	5	5	8	0.84	65.00	2.50	4	4	8.00	0.80	0.075	0.09
34	5008-2	6	5	5	8	0.84	60.00	2.50	4	4	8.00	0.87	0.082	0.10
35	5008-3	6	5	5	8	0.84	60.00	2.50	4	4	8.00	0.80	0.075	0.09
36	5008-4	6	5	2.5	8	0.84	65.00	2.50	2.5	3	9.00	1.07	0.101	0.10
37	15020-C	2	15	15	20	2.11	N/A	N/A	3	3	8.00	0.93	0.02	0.10
38	7520-C	4	7.5	7.5	20	2.11	N/A	N/A	3.2	4	13.00	1.13	0.034	0.02
39	5008-C	6	5	5	8	0.84	N/A	N/A	4	4	8.00	0.87	0.082	0.10

Note: due to large surface disturbance in Experiments 7520-4, 7510-4, and 15020-4, some quantities could not be measured, indicated N/A.

Table 4.2 Measured and Predicted Quantities for Experiments Conducted

Appendix B

<u>Figures</u>
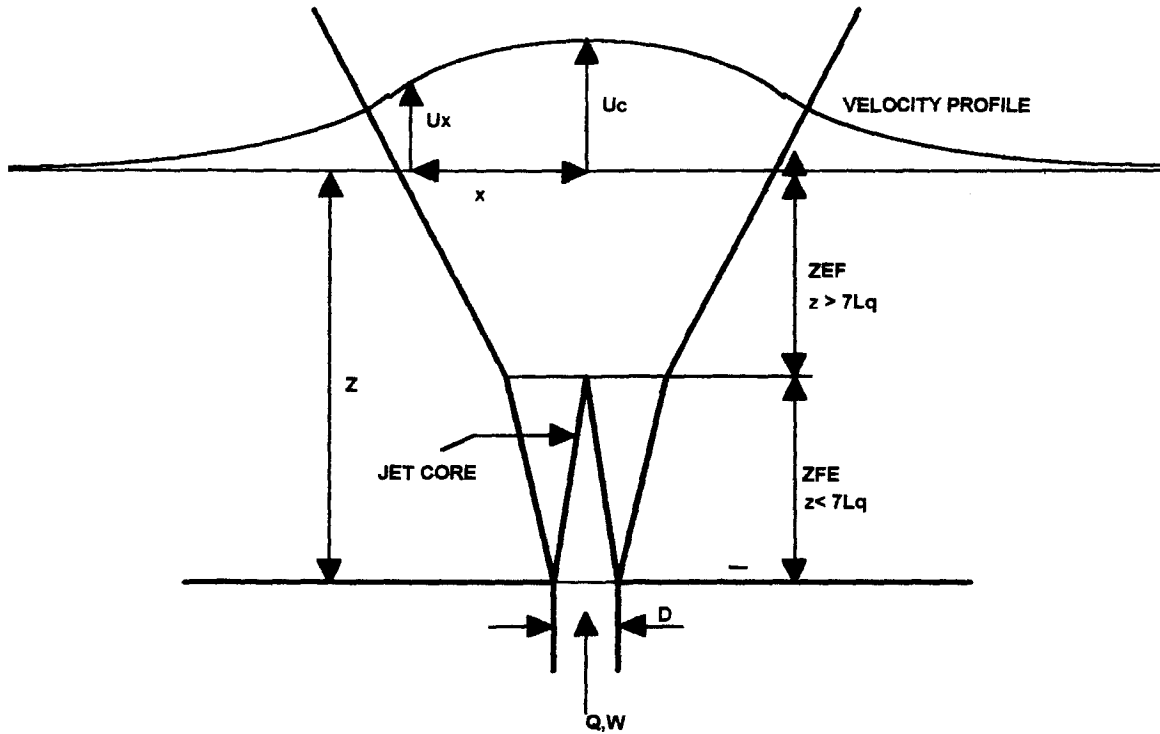
Figure 2.1   Definition sketch for pure round jets
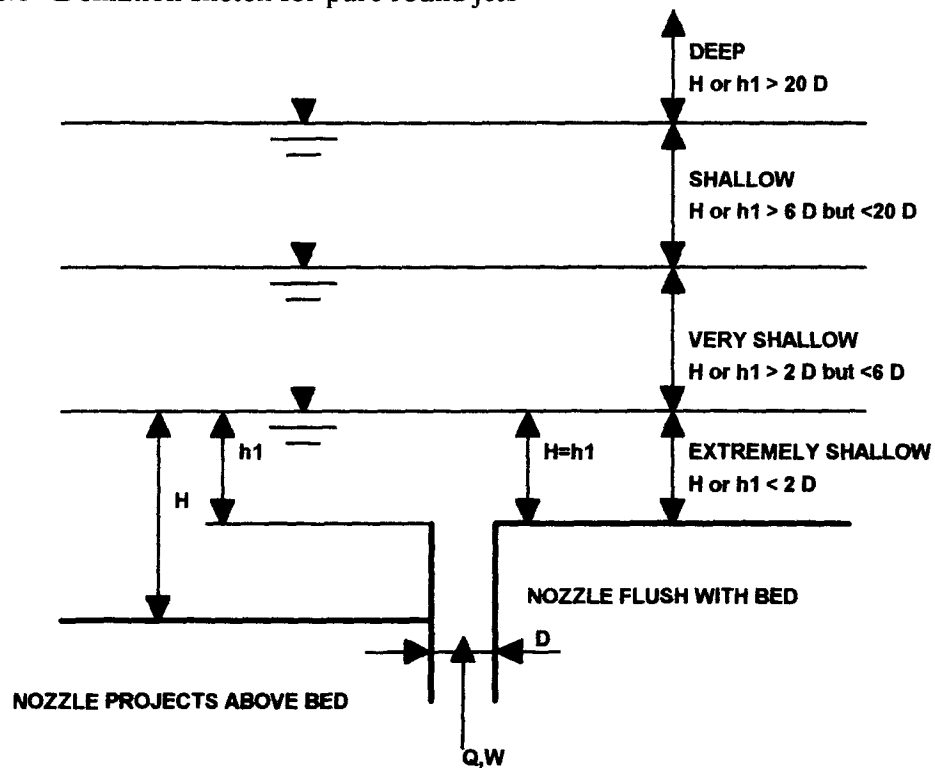
Figure 2.2   Defintition sketch for water depths

$$Z_t = z_t/D$$

ASYMPTOTIC VALUE OF A PLUME

Z_t

F_o
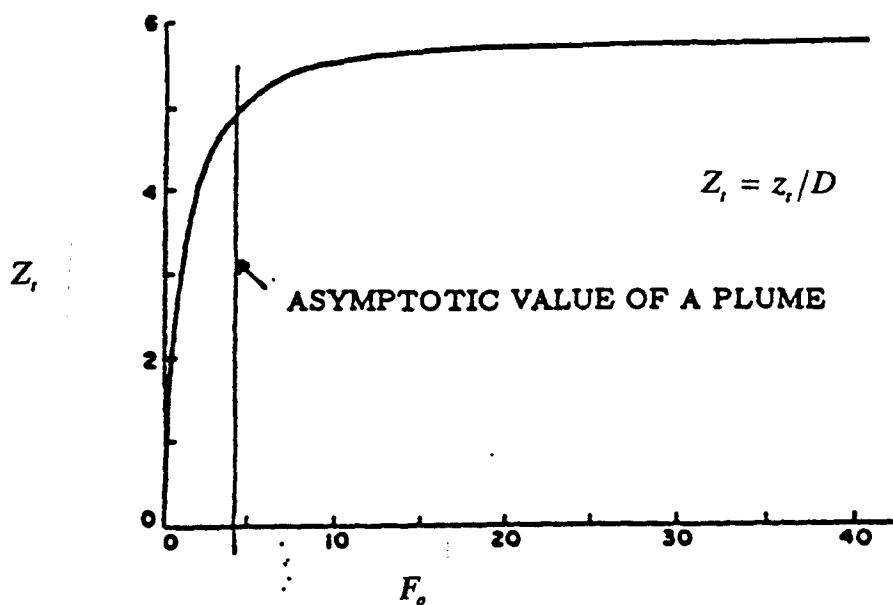
Figure 2.3 Length of Zone of Flow Establishment as a function of Source Densimetric Froude Number

FAR-FIELD   NEAR-FIELD

STRATIFIED COUNERFLOW REGION

SURFACE IMPINGEMENT REGION

RADIAL INTERNAL HYDRAULIC JUMP REGION

VERTICAL BUOYANT JET REGION

z

H

D

Q, W
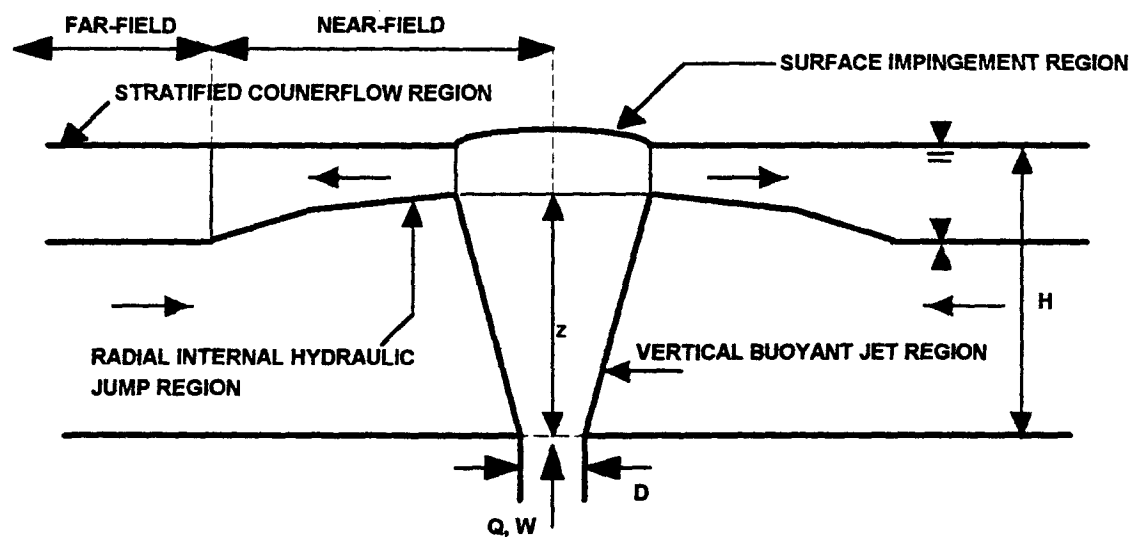
Figure 2.4 Regions of flow of a vertical buoyant jet in shallow water, according to Lee & Jirka (1981)
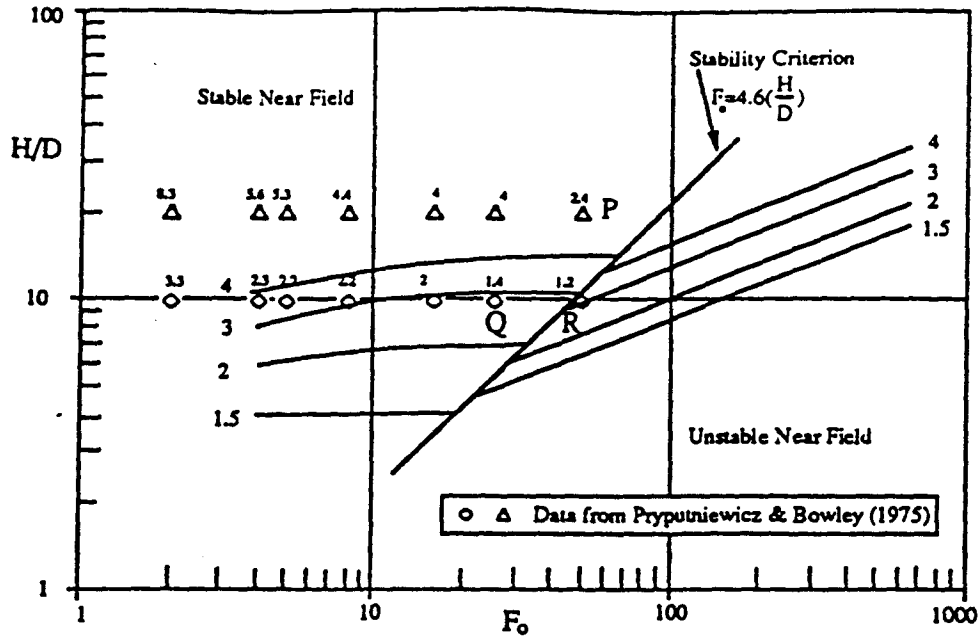
Figure 2.5 Stability Diagram, Lee & Jirka (1981)
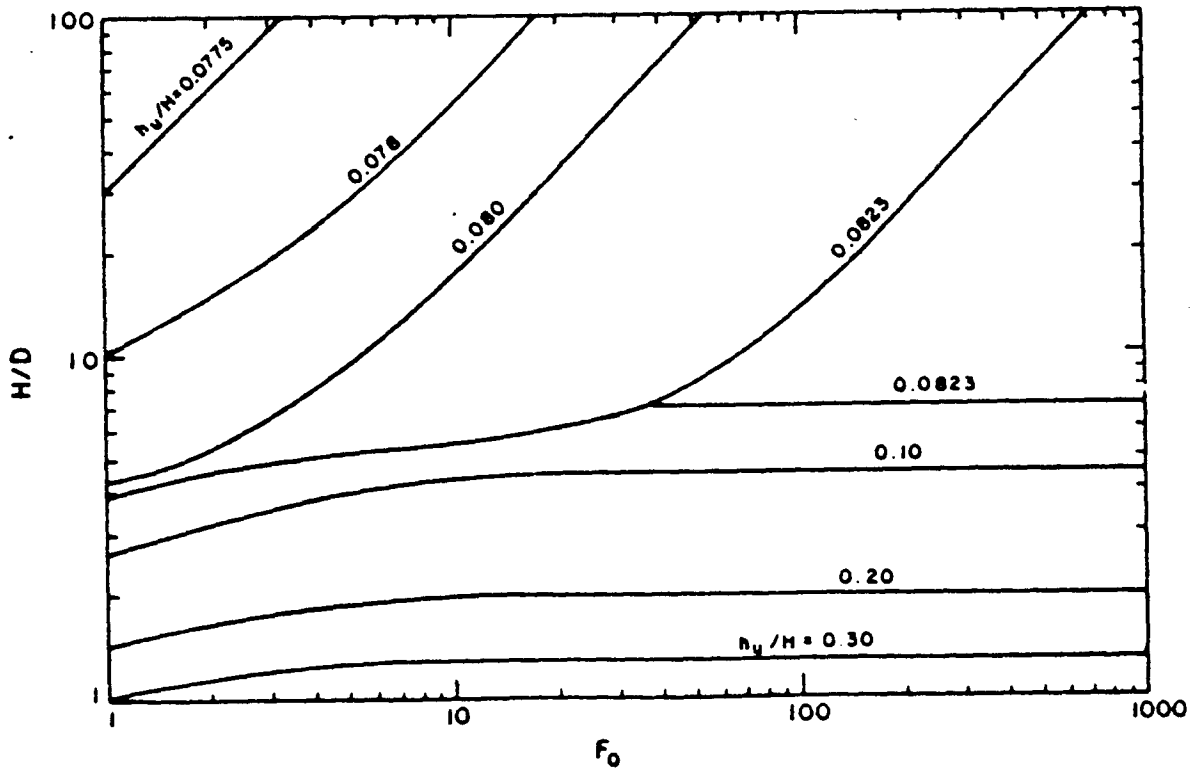
Figure 2.6 Thickness of surface impingement zone as a function of Source Densimetric
Froude Number, Lee & Jirka (1981)
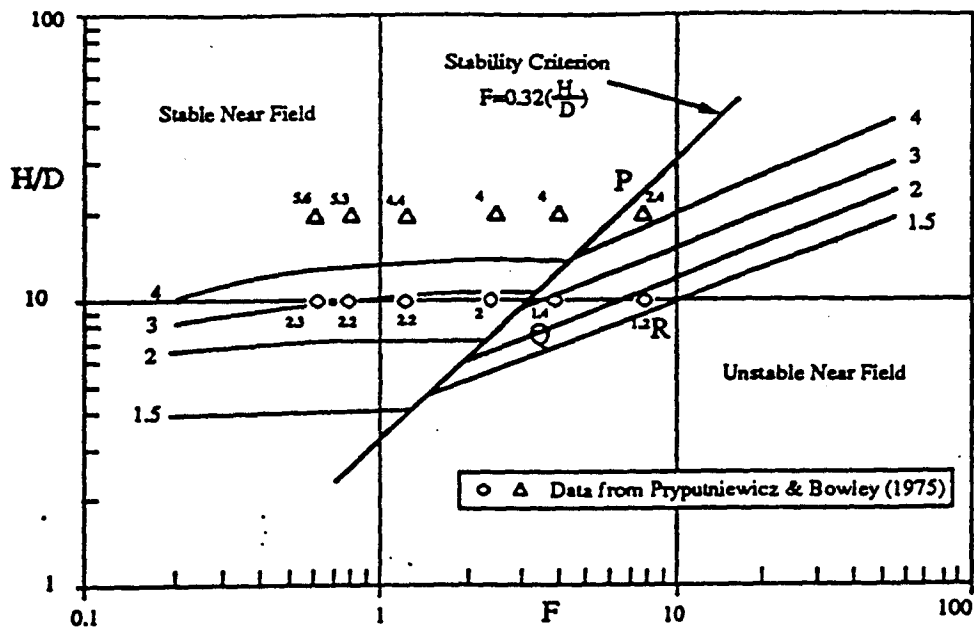
Figure 2.7   Stability diagram re-expressed in terms of F, Labridis (1989)
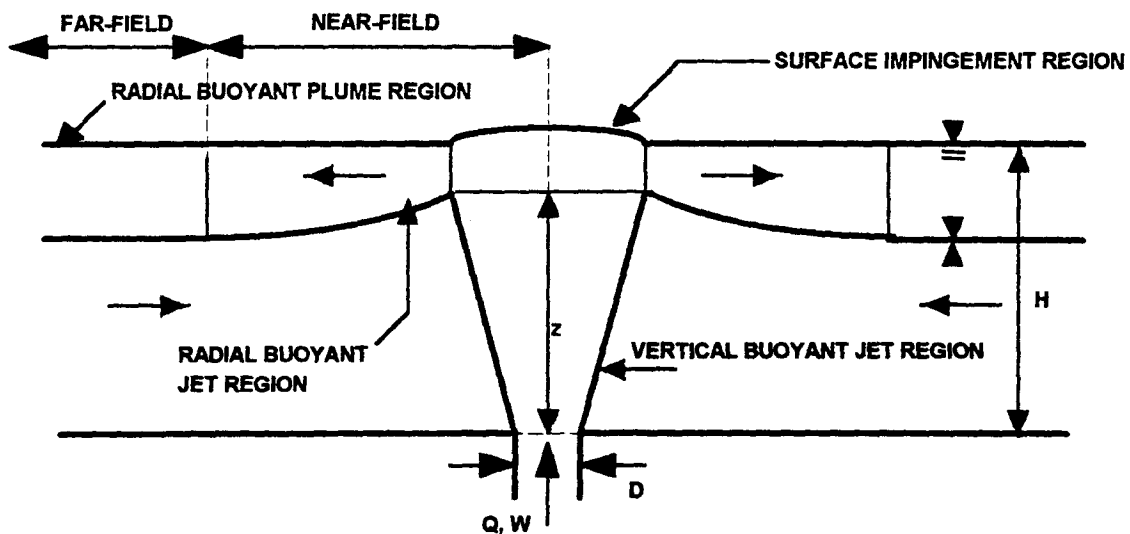
Figure 2.8   Flow regions of a vertical buoyant jet in shallow water, as defined by
Lawrence and Bratkovitch (1993)
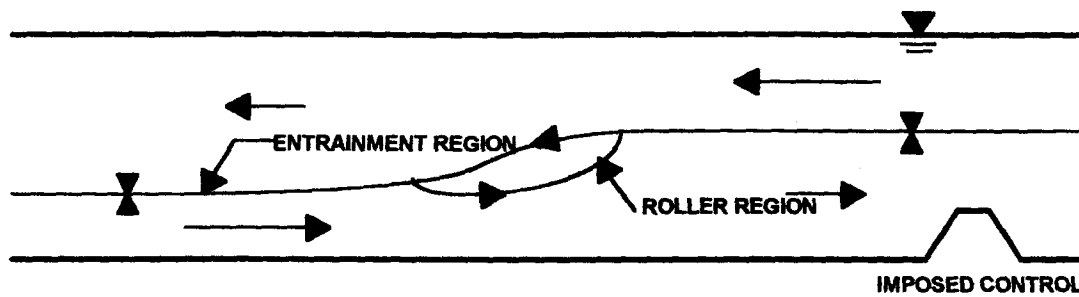
Figure 2.9 Internal hydraulic jump in a two layer flow in a channel, after Wilkinson &
Wood (1971)
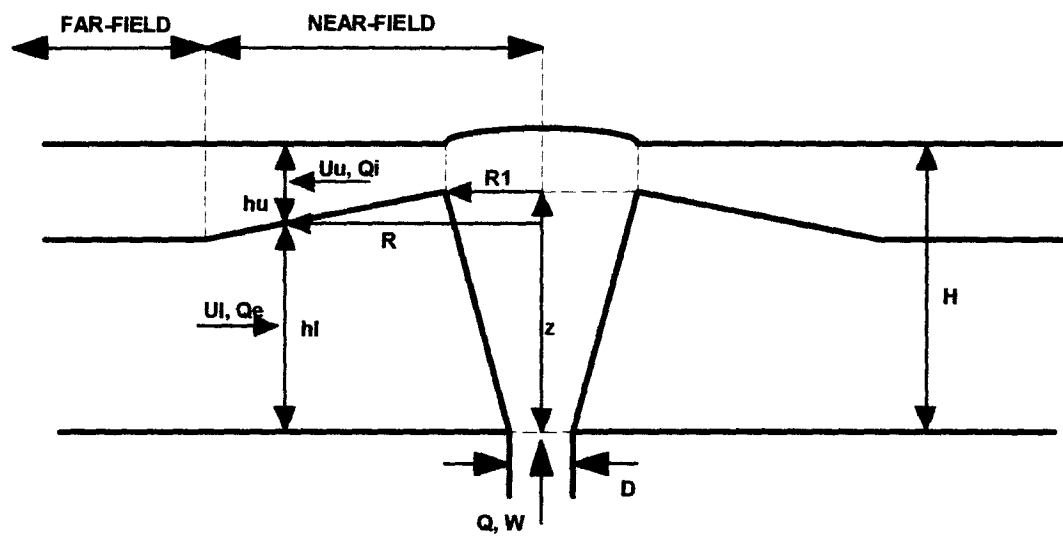
Figure 3.10 Definition sketch for flow prediction calculations
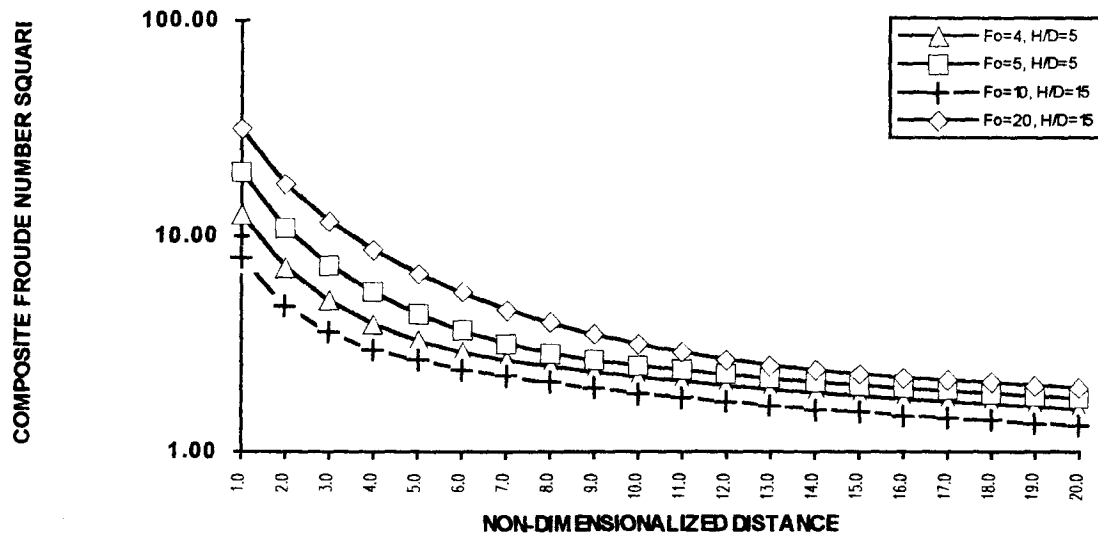
Figure 3.11A   Variation of Composite Froude Number Squared with Non-
Dimensionalized Radius
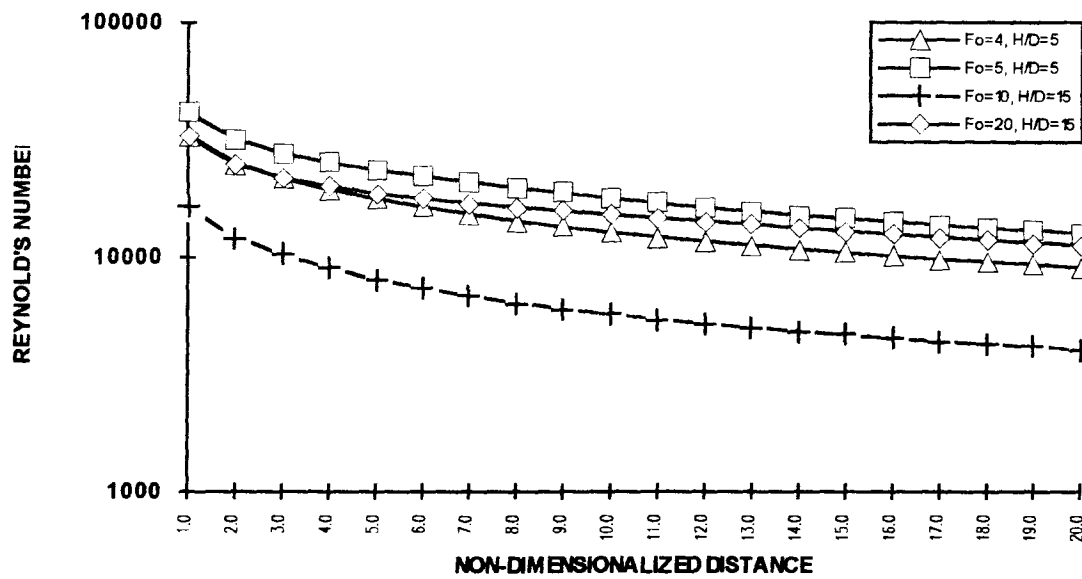
Figure 3.11B   Variation of Upper Layer Reynold's number with Non-Dimensionalized
Radius
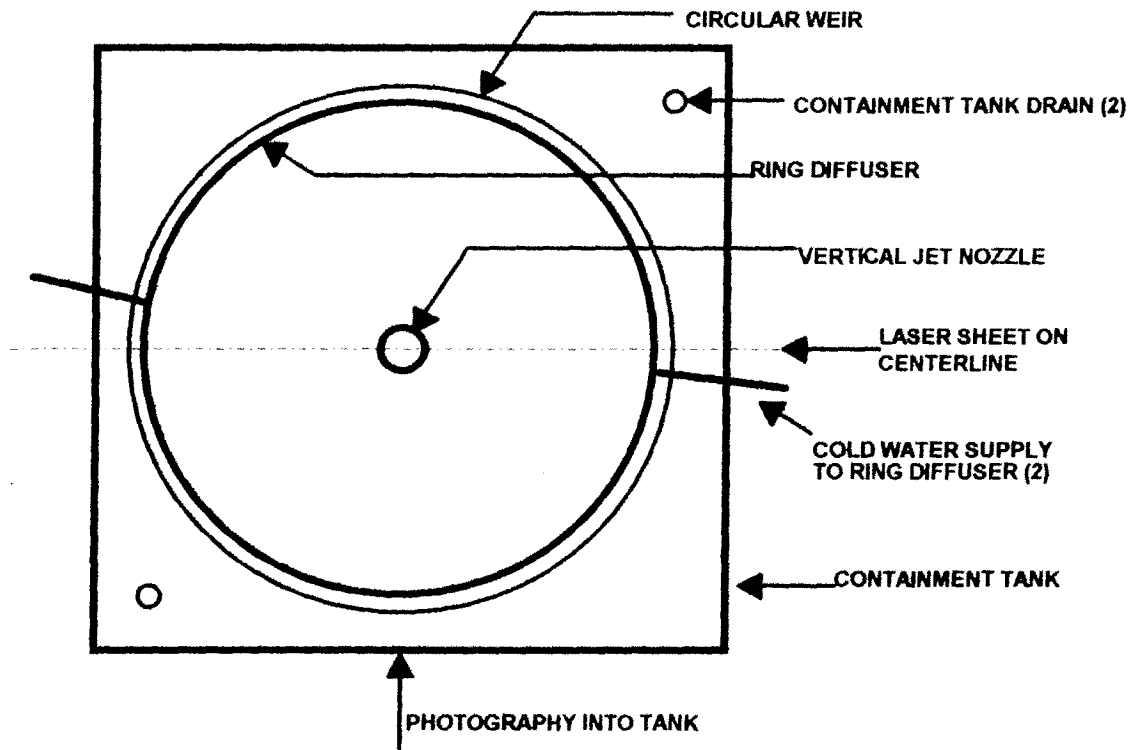
Figure 3.12 Plan view schematic of experimental apparatus
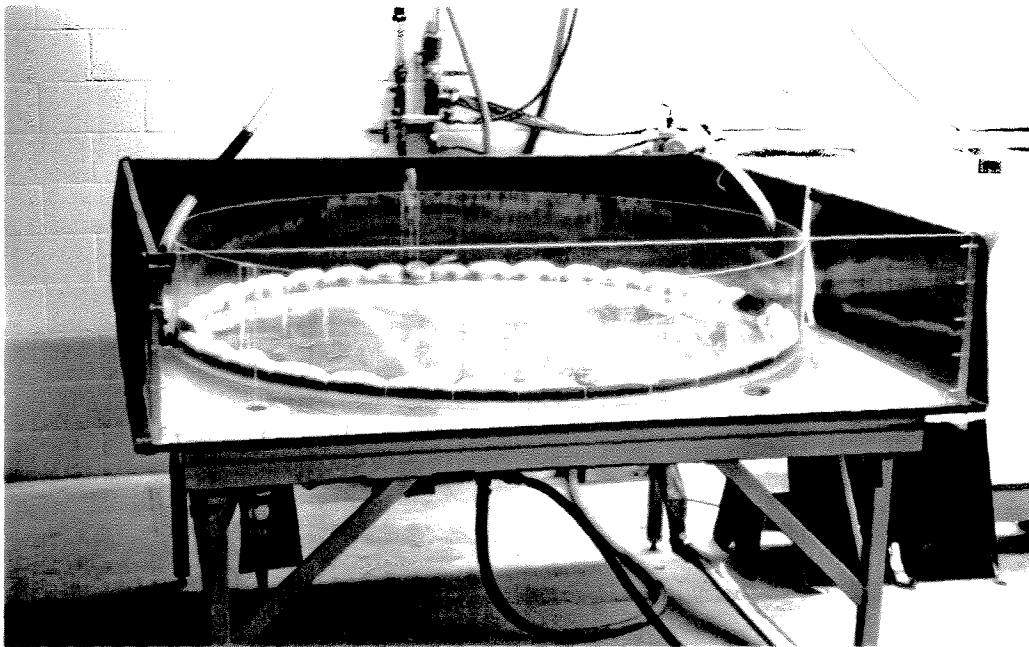
Figure 3.13 Photograph showing experimental apparatus
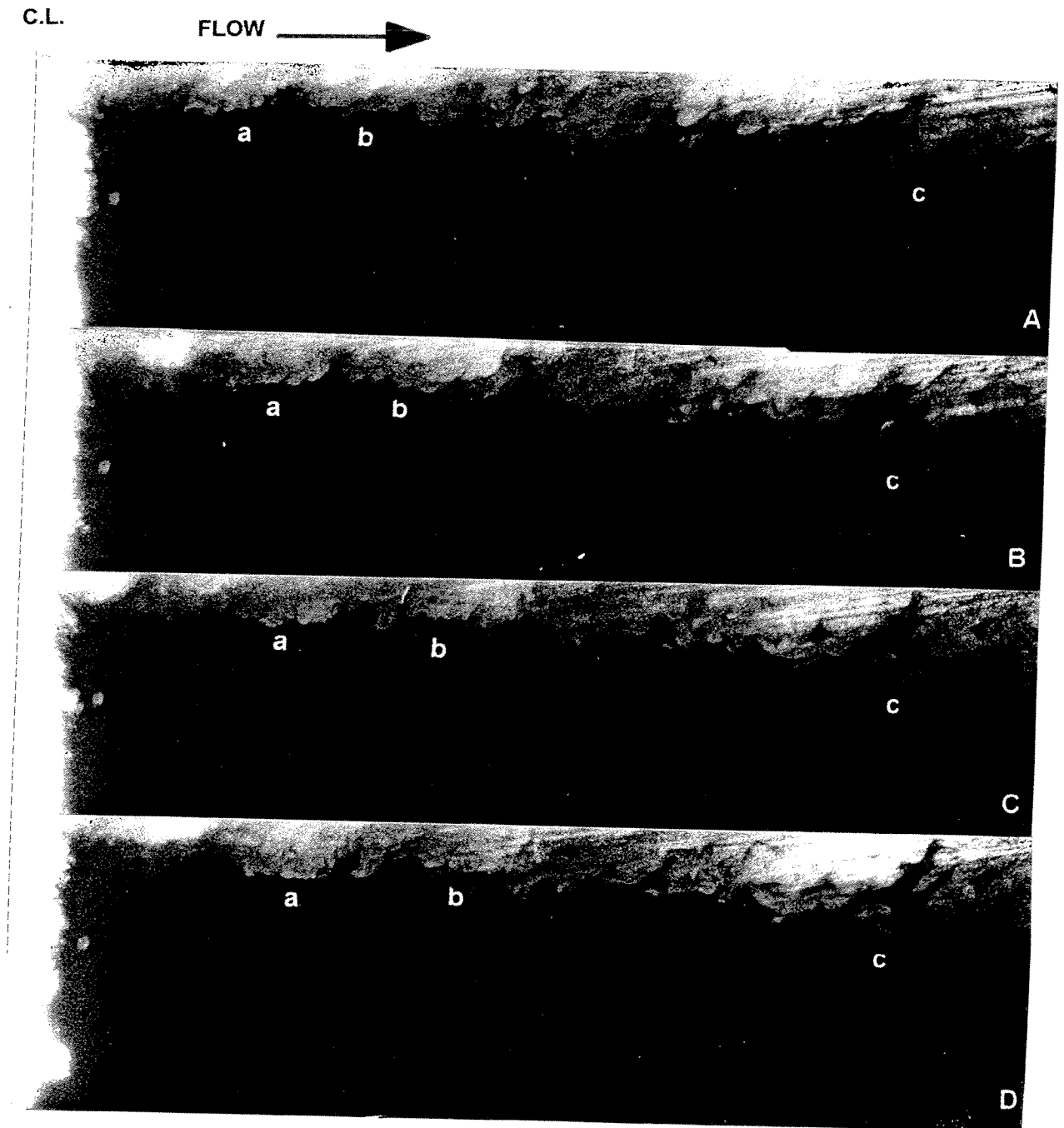
Figure 4.14 A-D   Surface flow of Experiment 15020-2.
Time interval 0.7s, approximate scale 1cm = 5 cm.
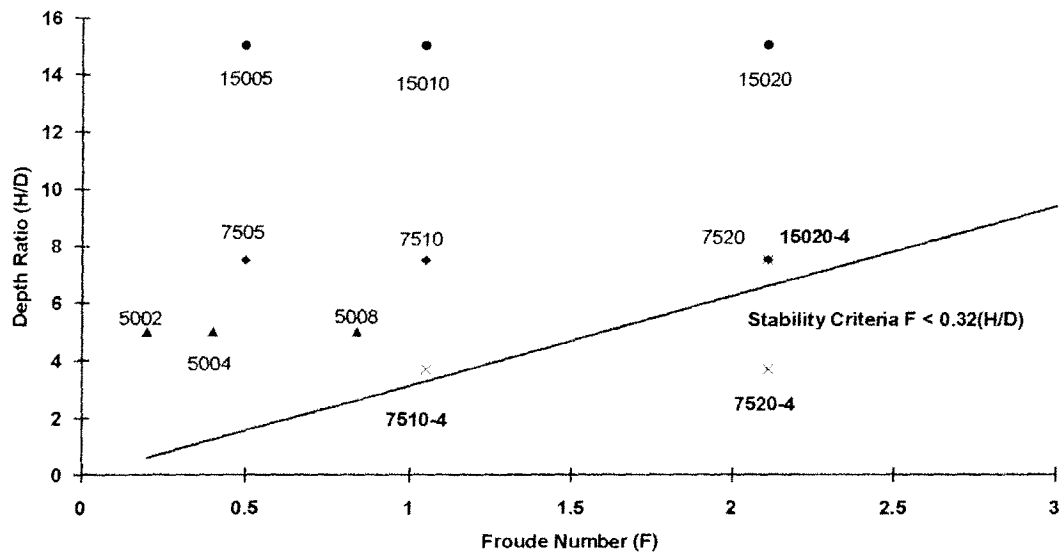
Figure 4.15 Comparison of experiments to stability criteria of Labridis (1989)
Experiments where plunge ring structure occurred plotted seperately, and
indicated in bold face.
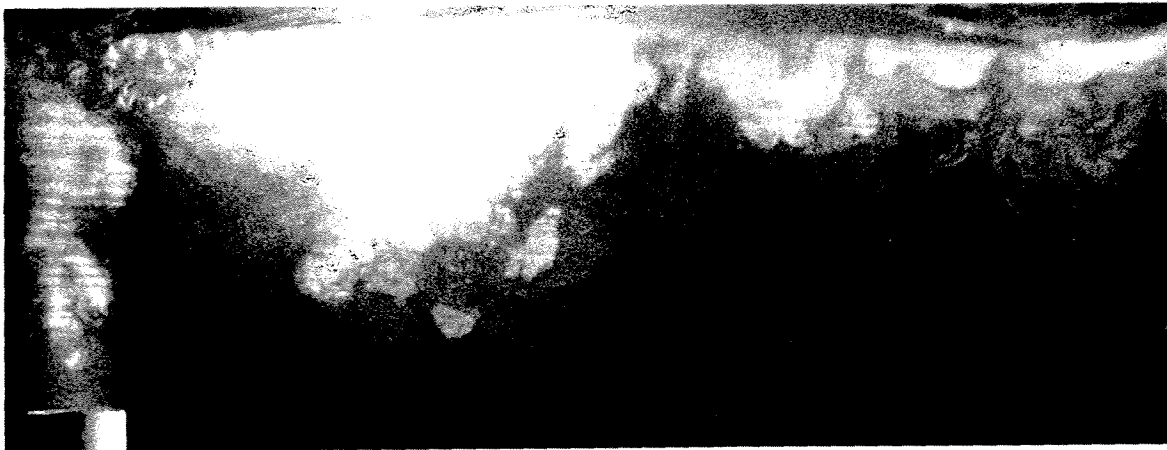
Figure 4.16 Plunging structure at the exit from surface impingement zone in Experiment
7520-4. Approximate scale 1cm = 3 cm.

Figure 4.17 A-D   Surface flow under choked conditions, Experiment 15020-C.
Time interval 0.7s, approximate scale 1cm = 5cm
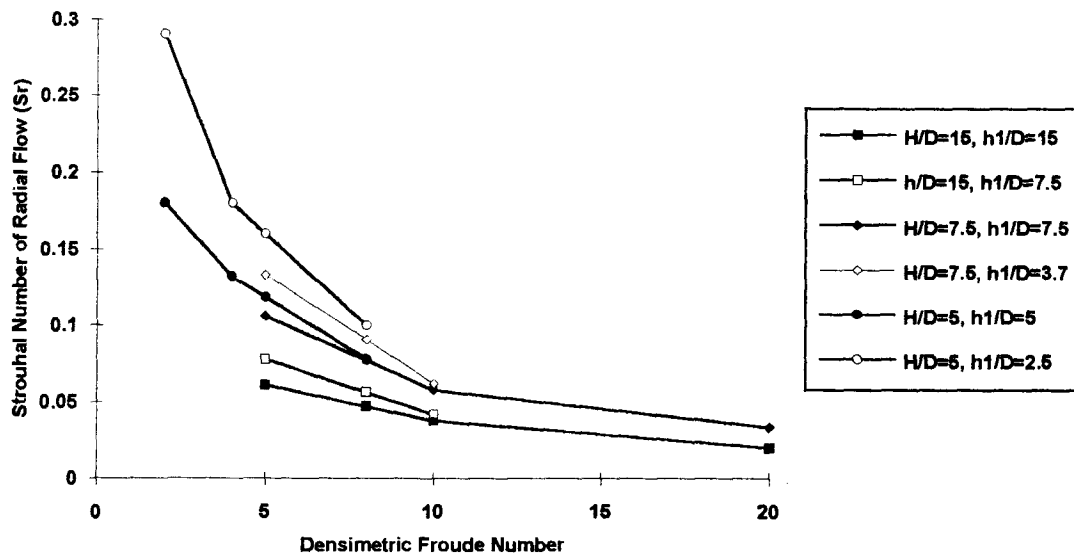
Figure 4.18 Variation of Strouhal number of radial flow with F_o
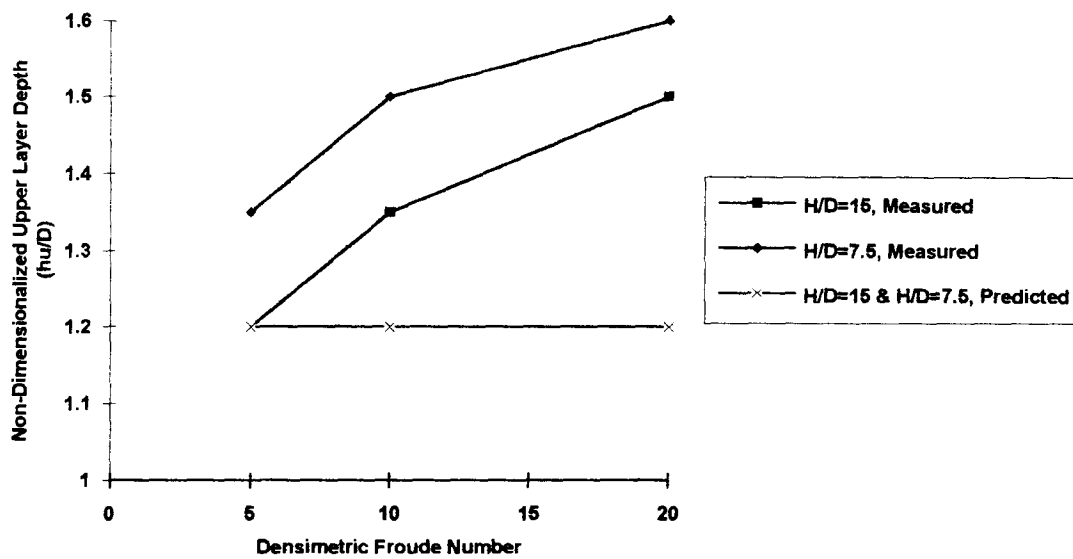
Figure 4.19 Non-dimensionalized measured upper layer depths vs F_o,
including values predicted using solutions of Lee & Jirka (1981)
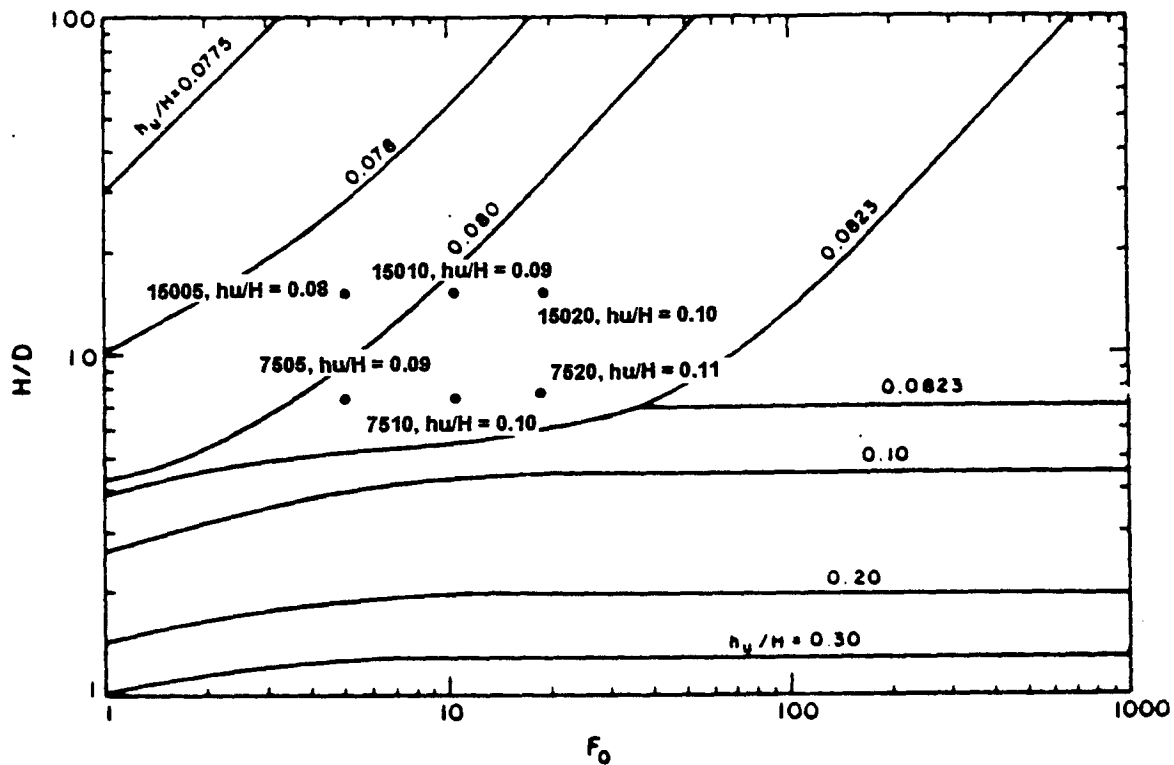
Figure 4.20 Comparison of observed upper layer depths with solutions of Lee & Jirka, (1981). Upper layer depth non-dimensionalized by dividing by H. Solutions of Lee & Jirka in solid lines. Data this study indicated: • **expt. series, hu/H =** upper layer depth divided by H, e.g • **7505, hu/H=0.09**
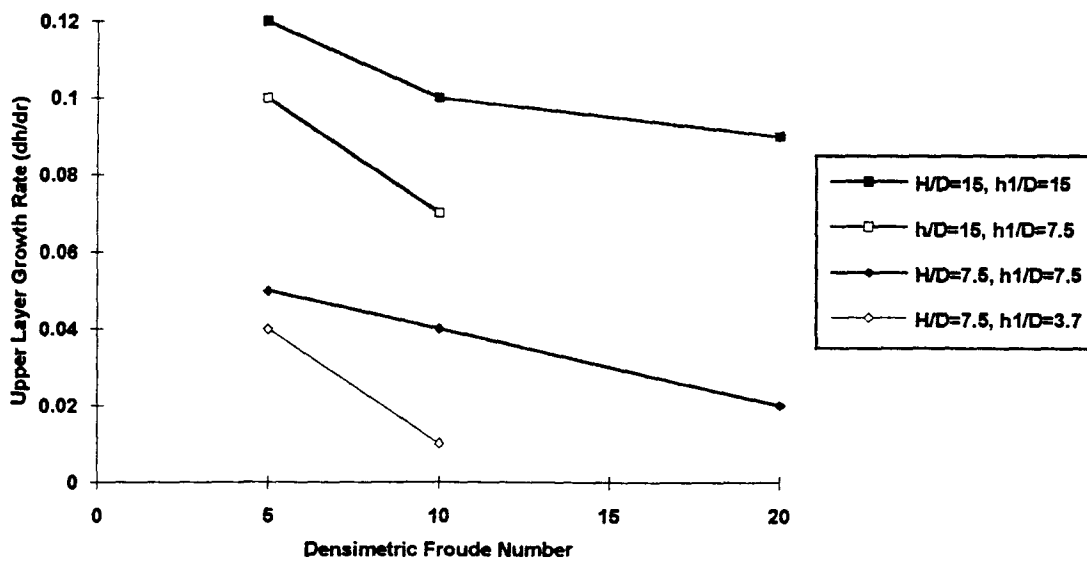

Figure 4.21 Variation of upper layer growth rate with F_o
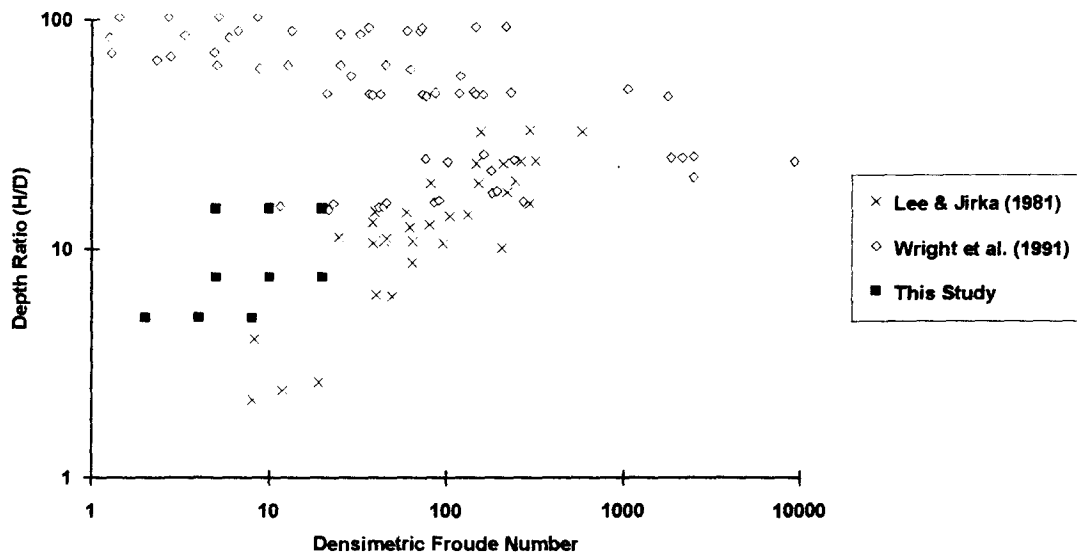
Figure 4.22 Comparison of range of experiments of Lee & Jirka (1981), Wright et al. (1991), and this study.